

1    **Osteology and neuroanatomy of a Miocene phasianid (Aves:  
2    Galliformes) from the Miocene of Nebraska**

3    Daniel T. Ksepka<sup>1\*</sup>, Catherine M. Early<sup>2</sup>, Kate Dzikiewicz<sup>1</sup>, and Amy M. Balanoff<sup>3</sup>

4

5    <sup>1</sup>Bruce Museum, Greenwich, Connecticut 06830, USA <dksepka@brucemuseum.org>

6    <sup>2</sup>Biology Department, Science Museum of Minnesota, Saint Paul, Minnesota 55102, USA

7    <cearly@smm.org>

8    <sup>3</sup>Department of Psychological and Brain Sciences, Johns Hopkins University, Baltimore,

9    MD, 21218, USA <abalano2@jhu.edu>

10

11

12

13    **Running Header: Miocene fossil phasianid**

14 **Abstract.**— Tetraoninae (grouse) and Meleagridinae (turkeys) are conspicuous  
15 representatives of the modern North American avifauna. The pre-Pleistocene fossil record  
16 of these clades has historically been limited to fragmentary remains, in some cases  
17 contributing to confusion rather than improving our understanding of how these charismatic  
18 landfowl evolved. We report an exquisitely preserved partial skeleton representing a new  
19 species of Late Miocene phasianid from the Ash Hollow Formation of Nebraska.  
20 *Centuriavis lioae* is a phasianid species close in size to modern sage-grouse that diverged  
21 prior to the grouse-turkey split and thus offers insight into the early history of this radiation.  
22 The cranial endocast resembles other North American phasianids and differs from  
23 odontophorids in exhibiting a strongly projected Wulst bordered by a well-defined  
24 vallecula. Phylogenetic analyses indicate that *Centuriavis lioae* gen. et sp. nov. forms a  
25 clade with Tetraoninae, Meleagridinae, and *Pucrasia macrolopha* (Koklass pheasant). The  
26 new fossil species provides a late Miocene minimum calibration for the divergence of these  
27 extant taxa from other Galliformes and supports the hypothesis of a single dispersal from  
28 Asia to North America by a lineage that later gave rise to grouse and turkeys.  
29  
30 UUID: <https://zoobank.org:34ecda2f-f2f2-4c92-a82f-292e23cf2da1>

31     **Introduction**

32

33     Phasianidae represent the most species-rich and morphologically diverse radiation of  
34     Galliformes (landfowl or gamebirds) (del Hoyo et al., 1994). This family includes  
35     pheasants, Old World quails, partridges, peafowl, grouse, and turkeys. North America is  
36     today inhabited by two native phasianid clades, the Meleagridinae (turkeys) and the  
37     Tetraoninae (grouse). Several other phasianid species, including *Phasianus colchicus*  
38     (Common Pheasant) and *Alectoris chukar* (Chukar) have been introduced by humans in  
39     historical times and established breeding populations. Aside from Phasianidae, two other  
40     families of Galliformes also occur in North America today: the Odontophoridae (New  
41     World quail) and Cracidae (chachalacas, guans, and curassows).

42         Meleagridinae are distinctive birds that are easily identified by their large size, bare  
43         heads, and iridescent plumage. Today the clade is represented by just two species,  
44         *Meleagris gallopavo* (Wild Turkey) and the *Meleagris ocellata* (Ocellated Turkey) (placed  
45         in the separate genus *Agriocharis* in some earlier taxonomies). Tetraoninae are widespread  
46         throughout the Holarctic and represented by 19 extant species, 12 of which occur in North  
47         America (Gill et al., 2021). These species range in size from the small ptarmigans to the  
48         impressive capercaillies, and share various adaptations to cold winter conditions including  
49         feathered nostrils and feathered and/or pectinate toes that aid in traveling atop snow.

50         The phylogenetic relationships of Meleagridinae and Tetraoninae have been the  
51         subject of substantial debate. Some early taxonomies depicted turkeys and grouse as  
52         successive branches on the galliform tree (e.g., Johngard, 1986), whereas others placed  
53         them in their own families separate from Phasianidae (Meleagrididae and Tetraonidae; e.g.

54 Porter, 1994; de Juana, 1994). Somewhat surprisingly, previous phylogenetic analyses  
55 based on morphological data failed to support a sister-group relationship between these two  
56 rather similar groups of birds (Dyke et al., 2003; Ksepka, 2009). Early molecular analyses  
57 based on DNA hybridization (Sibley and Alhquist, 1990) and mitochondrial DNA  
58 supported a sister-group relationship between grouse and turkeys (Kimball et al., 1999;  
59 Dimcheff et al., 2002), but subsequent studies based on larger sequence samples recovered  
60 alternate topologies (Crowe et al., 2006; Kan et al., 2010). Most recently, molecular  
61 phylogenetic analyses have converged on a topology supporting a sister-group relationship  
62 between Meleagridinae and Tetraoninae, suggesting they shared a relatively recent  
63 common ancestor, and possibly split from one another following a dispersal event into  
64 North America (Kriegs et al., 2007; Kaiser et al., 2007; Kimball and Braun, 2008; Kimball  
65 et al., 2011; Wang et al., 2013; Hosner et al., 2017). Most recent work suggests that the  
66 closest living relative of the turkey + grouse clade is the Koklass pheasant *Pucrasia*  
67 *macrolopha*, a modest-sized bird that ranges throughout high-altitude forests in the  
68 Himalayas and China (Wang et al., 2013; Hosner et al., 2017).

69

70 *Fossil record of North American Galliformes*.—Until now, the fossil record has  
71 offered little insight into the early evolution of the turkey + grouse clade. Interestingly, the  
72 earliest records of North American landfowl appear to belong to stem taxa, revealing that at  
73 least one colonization of the continent ultimately ended in extinction, followed by later  
74 more successful arrivals of Cracidae, Odontophoridae, and Phasianidae. The oldest putative  
75 record of Pan-Galliformes is the Late Cretaceous *Austinornis latus* (Marsh, 1877;  
76 Shufeldt, 1915; Clarke, 2004). However, this taxon is known only from a partial

77 tarsometatarsus and its phylogenetic position is best considered uncertain pending better  
78 material (Mayr, 2016a). Complete skeletons of the stem landfowl species *Gallinuloides*  
79 *wyomingensis* from the Early Eocene Green River Formation of Wyoming provide more  
80 definitive records. *Gallinuloides* appears to have lacked skeletal accommodations for a  
81 large crop and shows no evidence of consuming gastroliths, suggesting it was not adapted  
82 to consuming the tough foodstuffs such as seeds favored by many modern landfowl (Mayr  
83 and Weidig, 2004).

84 Several Eocene and Oligocene fossils were formerly assigned to crown Galliformes  
85 but now appear to represent stem taxa. *Procrax brevipes* from the Late Eocene of South  
86 Dakota is known from a single nearly complete skeleton. Tordoff and Macdonald (1957)  
87 considered this taxon to be closely related to Cracidae, but its phylogenetic affinities are in  
88 need of re-appraisal and it likely represents another stem member of Pan-Galliformes  
89 (Mayr, 2009). *Archaealectrornis sibleyi* is known only from a humerus from the early  
90 Oligocene of South Dakota, which lacks the distal projection of the caput humeri that  
91 separates the incisura capitis and fossa tricipitalis dorsalis in all extant Galliformes (Crowe  
92 and Short, 1992). This species thus likely also belongs outside crown Galliformes (Mayr,  
93 2009). *Palaeonossax senectus* was based on the distal end of a humerus from the Upper  
94 Oligocene Brule Formation of South Dakota. Wetmore (1956) considered the fossil to  
95 closely resemble the extant cracid *Ortalis vetula*, but at least as illustrated the specimen  
96 shows no obvious derived features of Cracidae and the orientation of the distal condyles  
97 raises doubts over whether it even belongs to a galliform bird. The fossil record of stem  
98 landfowl from North America otherwise consists of taxa based on very limited material  
99 (reviewed in Stidham et al., 2020).

100           Discounting dubious records discussed above, Cracidae have their earliest record in  
101       the Miocene of Florida (Olson and Farrand, 1974). Multiple cracid species have been  
102       described from sparse material from the Miocene and Pliocene of California, Kansas,  
103       Florida, South Dakota, and Nebraska. All were assigned to the genus *Boreortalis* by  
104       Brodkorb (1964), though this taxonomic decision was considered arbitrary by Olson  
105       (1985).

106           A partial skull from the latest Eocene or earliest Oligocene of Washington state  
107       appears to belong to an archaic member of Phasianoidea (Odontophoridae + Numididae +  
108       Phasianidae) (Mayr et al., 2021). If this phylogenetic placement is substantiated, the skull  
109       would be a contender for the oldest record of crown Galliformes in North America.

110           The fossil record of Odontophoridae is in need of major revision. The oldest alleged  
111       record of Odontophoridae, *Nanortyx inexpectus* from the Eocene of Canada (Weigel, 1963),  
112       most likely represents the stem landfowl clade Quercymegapodiidae (see Mourer-Chauviré  
113       1992). The distal end of a putative odontophorid tarsometatarsus from the Oligocene of  
114       Colorado was described but not figured by Tordoff (1951). Re-examination of this  
115       specimen is necessary to establish the affinities of this fossil, which may prove simply too  
116       incomplete to assign to any family. Fragmentary material from the Miocene of California  
117       and South Dakota assigned to Odontophoridae is likewise best treated with skepticism (see  
118       Olson, 1985). *Miortyx terres* from the early Miocene of South Dakota was assigned to  
119       Odontophoridae based primarily on the deep fossa tricipitalis dorsalis by Miller (1944).  
120       Howard (1966) later described a fragmentary humerus from the early Miocene of South  
121       Dakota as *Miortyx aldeni*, also based on the deep fossa tricipitalis dorsalis. This humerus,  
122       however, is 50% larger than the holotype humerus of *Miortyx terres*, and falls well outside

123 the size range of extant Odontophoridae. Given the large size of *Miortyx terres*, the fact that  
124 a deep fossa tricipitalis dorsalis is present in many fossil taxa such as *Palaeortyx*, and the  
125 distinct shape of the incisura capititis of *Miortyx* (which is unlike that in any extant New  
126 World quail), it is possible that this genus is non-monophyletic and that one or both species  
127 fall outside Odontophoridae. Abundant skeletal material from the Pliocene of Florida,  
128 including skulls, has been assigned to the extant *Colinus virginianus* (Northern Bobwhite)  
129 (Emslie, 1998), marking the earliest confirmed record of Odontophoridae in North America  
130 pending re-examination of older fragmentary fossils.

131 The North American record of Phasianidae comprises a number of taxa assigned to  
132 Tetraoninae and Meleagridinae, along with some putative records that are best considered  
133 Galliformes *incertae sedis*. One often-overlooked taxon is *Archaeophasianus*, a former  
134 contender for the oldest record North American of Phasianidae. Shufeldt (1915) described  
135 two fossil species, which he assigned to the extant genus *Phasianus*: *Phasianus*  
136 *americanus*, based on a partial tarsometatarsus and pedal phalanx collected from the  
137 Middle John Day of Paulina Creek, Oregon (misspelled as “Parilina Creek” in the original  
138 description, see Brodkorb, 1964) and *Phasianus mioceanus*, based on a partial humerus  
139 from Scott’s Bluff, Nebraska and a partial femur from Chimney Rock, Nebraska. Stone  
140 (1915) noted this name was preoccupied by *Phasianus americanus* Audubon 1839 and  
141 proposed the new species name *Phasianus roberti*. Subsequently, Lambrecht (1933) erected  
142 the genus *Archaeophasianus* to accommodate these two species, in recognition of their  
143 distinctness from *Phasianus*. Brodkorb (1964) considered the genus to belong to  
144 Tetraoninae.

145 The precise stratigraphic horizon from which the *Archaeophasianus roberti*  
146 holotype was collected is uncertain. Shufeldt (1915) considered it Oligocene in age.  
147 Brodkorb later (1964) attributed it without explanation to the Upper Miocene Mascall  
148 Formation, whereas Fremd (2010) attributed it to beds A-D of the Turtle Cove assemblage  
149 of the John Day, indicating a latest Oligocene age. *Archaeophasianus mioceanus* is  
150 considered to be Miocene in age, but the precise stratigraphic horizon is again uncertain.  
151 Brodkorb (1964) attributed the co-types to the Sheep Creek or Marsland Formation,  
152 without comment. Whether *Archaeophasianus roberti* and *Archaeophasianus mioceanus*  
153 should be assigned to a single species cannot be adequately evaluated, as no overlapping  
154 elements are preserved for both species. Like *Archaealectrornis sibleyi*, the humerus of  
155 *Archaeophasianus mioceanus* lacks the distal projection of the caput humeri that  
156 characterizes extant Galliformes, and the incisura capitis and fossa tricipitalis dorsalis are  
157 instead separated only by a weak ridge. This suggests *Archaeophasianus mioceanus* may  
158 fall not only outside Phasianidae, but also outside of crown Galliformes.

159 The oldest reported fossil record of the turkey lineage is *Rhegminornis calobates*,  
160 based on a partial tarsometatarsus from the Miocene Thomas Farm locality of Florida.  
161 Originally considered a shorebird (Wetmore, 1943), this species was re-identified as a  
162 turkey by Olson and Farrand (1974). Steadman (1980:140), in a major review of the turkey  
163 fossil record, considered the material “insufficient to place it unequivocally within  
164 Meleagridinae, although such a placement may very well be correct”. Assignment of  
165 *Rhegminornis* to Meleagridinae relied in part on the presence of an “inner intertrochlear  
166 foramen” which opens between the bases of trochlea metatarsi II and III. This foramen is  
167 typically present in *Meleagris gallopavo*, but it is absent in several specimens of *Meleagris*

168 *ocellata* examined during the present study. Further, this foramen occurs in at least some  
169 individuals of *Pucrasia macrolopha*, *Perdix perdix*, and *Polyplectron inoptinatum*. Upon  
170 re-examination of the material, we failed to find a strong resemblance to modern turkeys,  
171 and consider assignment to Meleagridinae poorly founded.

172 *Proagriocharis kimballensis* is another small fossil species identified as a turkey.  
173 Martin and Tate (1970) named the species based on two coracoids and three tarsometatarsi  
174 in varying states of completeness. Originally considered Late Pliocene in age, the holotype  
175 and referred specimens were since re-dated to the Miocene (Olson, 1985). *Proagriocharis*  
176 can confidently be assigned to at least Phasianidae, though the paucity of material raises  
177 uncertainty about its placement in Meleagridinae and it is worth considering the possibility  
178 that this taxon may instead represent a stem member of the turkey + grouse clade. This  
179 issue will likely remain unresolved until better material surfaces.

180 All remaining turkey fossils are presently assigned, at least tentatively, to the extant  
181 genus *Meleagris*. The oldest of these is a large tibiotarsus from the Late Miocene of  
182 Virginia considered cf. *Meleagris* by Steadman (1980). Valid extinct species include the  
183 Late Pliocene *Meleagris leopoldi* from Texas (with possible additional records from  
184 Florida), the Early Pleistocene *Meleagris anza* from California, and the Late Pleistocene  
185 *Meleagris crassipes* from New Mexico. It is debatable whether *Meleagris progenes*, known  
186 from the Pliocene of Kansas and possibly also Arizona, represents an additional distinct  
187 species or a synonym of *Meleagris leopoldi* (see Stidham, 2011). By far the most well-  
188 known fossil turkey, however, is *Meleagris californicus*, which is abundant at the renowned  
189 Late Pleistocene Rancho La Brea site in California. This species appears to have ranged

190 throughout the western United States before being wiped out by a combination of regional  
191 aridification and hunting by humans (Bocheński and Campbell, 2006).

192 The North American fossil record of grouse remains scrappy, and no pre-  
193 Pleistocene specimens can be confidently identified to an extant genus (Drovetski, 2003).  
194 Wetmore (1932) described a partial humerus from the Miocene of Nebraska as  
195 *Palaealectoris incertus*, assigning the species to Tetraonidae (equivalent to Tetraoninae).  
196 This assignment is doubtful however, as the fossa pneumotricipitalis dorsalis in this fossil is  
197 deeply excavated, unlike extant grouse. This, together with the very small size of the  
198 humerus (maximum head width 11.1mm), suggests *Palaealectoris* may instead be a close  
199 relative of *Palaeortyx*. Another poorly established taxon, “*Tympanuchus*” *stirtoni*, was  
200 based on a proximal portion of a tarsometatarsus from the Miocene of South Dakota  
201 (Miller, 1941). The material is insufficient to support this assignment and this fragmentary  
202 fossil is best considered Galliformes indet.. The only convincing fossil records of grouse  
203 thus come from the extant genus *Dendragapus*: *Dendragapus lucasi* and *Dendragapus gilli*  
204 from the Pleistocene of Oregon, along with some additional Pleistocene remains from  
205 California referred to the subspecies *Dendragapus gilli milleri* (see Jehl, 1969).

206 In this contribution, we describe a new species of phasianid from the Miocene of  
207 Nebraska. The holotype specimen was collected in articulation and preserves the skull,  
208 presacral vertebral series, partial synsacrum, and partial pectoral girdle and wings. We  
209 present a revised phylogeny of Galliformes along with comments on the neuroanatomy of  
210 Phasianidae based on virtual endocasts from the new fossil and several extant phasianid  
211 taxa.

212

213 *Geological setting*.— AMNH FARB 8629 was collected by the Skinner Expedition of 1932  
214 at the *Machaerodus* Quarry, a locality in Cherry County, Nebraska. The mammalian fauna  
215 from this quarry indicates a Clarendonian North American Land Mammal Age (NALMA)  
216 (Tedford, et al., 2004). The *Machaerodus* Quarry is located within the Merritt Dam  
217 Member of the Ash Hollow Formation (Ogallala Group), and represents a channel fill cut  
218 into the underlying Cap Rock Member. An ash layer overlies the fossiliferous layer from  
219 which the specimen was collected. This layer has traditionally been referred to as the  
220 *Machaerodus* Ash. However, Lander (2008) argued that the *Machaerodus* Ash is equivalent  
221 to the Davis Ash, observing that these two ash layers, previously considered separate, never  
222 occur in superposition even at sections within <1km proximity of one another. Provided  
223 the *Machaerodus* Ash and Davis Ash are indeed one and the same, an Ar<sup>40</sup>/Ar<sup>39</sup> age of 11.5  
224 +/- 0.1Ma obtained from the Davis Ash (Swisher, 1992) provides a hard minimum age of  
225 11.4Ma for the *Centuriavis lioae* holotype, which is also likely a close approximation for  
226 the actual age of the fossil.

227

228

## 229 **Materials and methods**

230

231 *Anatomical nomenclature*.— Osteological terminology follows Baumel & Witmer (1993)  
232 with additional terminology for the quadrate following Elzanowski et al., (2000).

233

234 *Computed tomography scanning and visualization*.— AMNH FARB 8629 was microCT  
235 scanned at the AMNH Microscopy and Imaging Facility at a resolution of 74.2 microns.

236 Virtual models of the brain endocast and quadrate of this specimen were generated by  
237 segmenting these structures in Avizo (Thermo Fisher Scientific, Waltham, MA, USA).  
238 Portions of the braincase were broken and slightly offset, as can be seen on the right  
239 cerebral hemisphere, or missing, as is the case with the rostral portion of the braincase  
240 ventral to the olfactory bulbs and dorsal to the hypophysis. In those areas, we created  
241 smooth connections between the preserved bones that approximated the shape of a  
242 galliform endocast without fabricating anatomy, following best-practices approaches  
243 outlined by Balanoff et al. (2016). For comparative purposes, we rendered endocasts from  
244 the skulls of three North American galliform species: the turkey *Meleagris gallopavo*  
245 (OUVC 10599, scanned at OUmicroCT at 47.2 micron resolution), the grouse *Bonasa*  
246 *umbellus* (AMNH SKEL 21616, scanned at AMNH Microscopy and Imaging Facility at  
247 34.9 micron resolution), and the odontophorid *Colinus virginianus* (AMNH SKEL 2310,  
248 scanned at AMNH Microscopy and Imaging Facility at 27.4 micron resolution). Endocasts  
249 for each of these specimens were generated using the same methods as for the fossil.  
250

251 *Body mass estimation*.— Field et al. (2013) reported that maximum coracoid length showed  
252 the strongest correlation to body mass in Galliformes. In order to estimate the body mass of  
253 the *Centuriavis lioae* holotype individual we utilized Field et al's (2013) regression:

254

$$255 \quad \ln(\text{mass}) = 3.06 (\ln \text{coracoid length}) - 5.11$$

256

257 This yielded a mass estimate of 1.718kg.

258

259 *Phylogenetic analyses*.— In order to resolve the phylogenetic placement of *Centuriavis*  
260 *lioae*, we scored the new taxon into the morphological data matrix of Ksepka (2009). We  
261 added 16 new characters and two additional fossil taxa, the possible stem phasianid  
262 *Palaeortyx gallica* and the recently described crown phasianid *Panraogallus hezhengensis*.  
263 The expanded matrix contains 136 characters based on osteology, soft tissue anatomy, and  
264 reproductive biology and samples seven outgroup species (Lithornithiformes,  
265 Tinamiformes and Anseriformes), 55 extant species of Galliformes, and five fossil species  
266 of Galliformes. A list of extant specimens examined for scoring the matrix is provided in  
267 Ksepka (2009). *Palaeortyx gallica* and *Panraogallus hezhengensis* were scored from the  
268 literature.

269 In order to constrain the relationships of extant taxa, we applied a backbone  
270 constraint topology based on the results of a recent ML analysis of 2,208,355 bp of  
271 molecular sequence data from 4,817 concatenated UCE loci by Hosner et al. (2017). The  
272 backbone constraint contains the 38 extant species that overlap between the Ksepka et al.  
273 (2009) matrix and the Hosner et al. (2017) tree. The positions of the remaining 25 extant  
274 species (and all fossil species) were unconstrained. Parsimony analyses were conducted in  
275 PAUP\*4.a168 (Swofford, 2002), using the heuristic search option and 10,000 replicates of  
276 random taxon addition with TBR branch swapping, with all characters equally weighted,  
277 multi-state codings treated as polymorphism, and branches of minimum length 0 collapsed.  
278 Instability in the position of *Panraogallus* resulted in poor resolution in the strict consensus  
279 tree, so we conducted an additional analysis with this taxon excluded.

280

281 *Repositories and institutional abbreviations*.—American Museum of Natural History  
282 (AMNH), New York, USA; Ohio University Vertebrate Collection (OUVC), Ohio, USA;  
283 Yale Peabody Museum of Natural History, New Haven, Connecticut, USA (YPM).

284

285 **Systematic Paleontology**

286 Aves Linnaeus, 1758

287 Galliformes Temminck, 1820

288 Phasianidae Horsfield, 1821

289 *Centuriavis* new genus

290 Figures 1, 2, 3

291

292 *Type species*.—*Centuriavis lioae*

293

294 *Diagnosis*.—*Centuriavis lioae* can be differentiated from other fossil and extant North  
295 American Galliformes by the following combination of features: absence of fenestra  
296 mandibularis caudalis (versus presence in Tetraoninae), presence of a large pneumatic fossa  
297 in the area of the impressio m. sternocoracoidei of the coracoid (absent in Gallinuloididae  
298 and Odontophoridae), shallow cotylaris scapularis (deep in Gallinuloididae, Paraortygidae,  
299 and *Procrax*), medially deflected acromion (straight in Meleagridinae and Tetraoninae),  
300 absence of pneumatic foramina on the scapula (a foramen is always present on the dorsal  
301 surface of the facies articularis humeralis in *Meleagris ocellata* and variably present in  
302 *Meleagris gallopavo*, whereas a foramen is present between the acromion and facies  
303 articularis humeralis in Tetraoninae), presence of a distal projection of the articular surface

304 of the caput humeri which forms a ridge separating the fossa pneumotricipitalis dorsalis  
305 from the incisura capitidis (absent in Gallinuloididae, Paraortygidae, and  
306 Quercymegapodiidae, separated by a faint ridge rather than a projection of the caput humeri  
307 in *Archaealectornis* and *Archaeophasianus*), and moderately deep fossa pneumotricipitalis  
308 dorsalis (shallow in *Archaeophasianus*, Cracidae, and Meleagridinae; extremely deep in  
309 *Miortyx* and Odontophoridae). Only the coracoid can be directly compared with  
310 *Proagriocharis*. This bone differs in having a proximo-distally elongate scapular cotyle  
311 (circular in *Proagriocharis*) and smaller size: coracoid length equals 60.6mm in  
312 *Centuriavis* versus 66mm to 67.2mm in *Proagriocharis* (range due to different estimates  
313 for the same slightly damaged specimen reported by Martin and Tate [1970] and Steadman  
314 [1980]). Although no elements overlap directly, *Centuriavis* can be differentiated by larger  
315 size from *Rhegminornis* (inferred to be ~70-85% the size of *Centuriavis* based on the  
316 coracoid: tarsometatarsus proportions of *Proagriocharis*).

317  
318 *Occurrence*.— Miocene of Nebraska.

319  
320 *Etymology*.—From the Latin centuria (one hundred) referencing the history of the fossil,  
321 which despite exceptional preservation remained undescribed for nearly a century.

322  
323 *Remarks*.—Although only a single species of *Centuriavis* is yet known, we divide the  
324 diagnosis into a genus level diagnosis comparing the new taxon to other North American  
325 Galliformes and a species diagnosis including finer level traits.

326

327

328 *Centuriavis lioae* new species

329 Figures 1, 2, 3

330

331 *Holotype*.—AMNH FARB 8629, articulated partial skeleton preserving the skull, presacral  
332 vertebral series, synsacrum, furcula, complete left and partial right coracoid, scapulae, right  
333 and left humerus, right radius, right ulna, right radiale, damaged right ulnare, and isolated  
334 sesamoid.

335

336 *Diagnosis*.—Two potential autapomorphies diagnose *Centuriavis lioae*: Sharp ventral  
337 deflection of the crista deltopectoralis and presence of a foramen in the depressio  
338 ligamentosa on the caudal face of the radius. We note that a similar foramen was present in  
339 a single specimen of *Meleagris gallopavo* (AMNH 18704), but absent in all other observed  
340 specimens of that species as well as all other galliform taxa surveyed for this study.

341

342 *Occurrence*.—Machaerodus Quarry, Cherry County, Nebraska. This quarry exposes the  
343 Late Miocene Merritt Dam Member of the Ash Hollow Formation (Ogallala Group).

344

345 *Description*.—The remarkably well-preserved skull is exposed in right lateral view (Fig. 1).  
346 The beak is shorter proportional to overall skull length than in *Meleagris* (beak length  
347 varies greatly among Tetraoninae). The tip of the beak is downturned, but not hooked. The  
348 nares are sub-ovoid with a taller caudal border, which is a result of the descending process  
349 of the nasal extending almost directly ventrally rather than slanting in a more rostroventral

350 direction. The nares are relatively small as in the grouse *Tympanuchus* and *Lagopus*,  
351 whereas the nares are more elongated in *Meleagris* and most other grouse (e.g.  
352 *Dendragapus*, *Tetrao* and *Bonasa*). A thin internarial bar is formed by the nasal processes  
353 of the premaxillae, which maintain a clear sutural contact throughout their length. Caudally,  
354 the premaxillae intervene between the frontals for a short distance. The frontals are wide  
355 between the orbits, and are deeply depressed at midline. The skull roof is generally smooth,  
356 lacking the rugosities developed along the margin of the orbit in some individuals of  
357 *Meleagris* and in *Tetraoninae*. As in most Galliformes, the cranial tip of the jugal is slightly  
358 dorsally deflected and abuts the caudal margin of the nasal, which creates a “notch”  
359 between the jugal and the freely projecting caudal end of the maxilla. Although the lacrimal  
360 head has been displaced, it is clear that the caudal border projected into the orbit forming a  
361 gently rounded supraorbital spine as in *Pucrasia* and *Tetraoninae* (sharper in  
362 *Meleagridinae*). In most members of Phasianidae, the processus postorbitalis is elongated  
363 and fuses with the ossified aponeurosis zygomaticus in adults (see Zusi and Livesey, 2000).  
364 Broken edges indicate that both of these delicate structures are missing their distal ends, so  
365 it is not possible to discern whether they were fused in *Centuriavis*. A contact between these  
366 structures cannot be identified on the left side of the skull in the CT data, but the processus  
367 zygomaticus shows an open break at the distal preserved margin, and so we consider the  
368 presence or absence of a contact to be uncertain.

369 The right quadrate is partially obscured because it remains in articulation, but it can  
370 be observed that the orbital process of the quadrate is elongate as in most Phasianidae, as  
371 opposed to the greatly shortened process in Odontophoridae. A well-developed tuberculum  
372 subcapitulare is present as in other Galloanserae. As in other representatives of Phasianidae,

373 the cotyla quadratojugal is has a strongly projected caudal margin, creating a deep socket for  
374 the quadratojugal (shallower in Odontophoridae). The left quadrate was digitally segmented  
375 from the CT scan data (Fig. 2), revealing that the capitulum oticum and capitulum  
376 squamosum are merged, a derived feature shared by Numididae, Odontophoridae, and  
377 Phasianidae. The scans also confirm the presence of a foramen pneumaticum rostromediale  
378 and absence of a pneumaticum caudomediale, as well as a bicondylar articulation for the  
379 mandible.

380 The mandible is more strongly downcurved than in *Meleagris*. As in other  
381 Phasianidae the symphysis is short. A fenestra mandibularis caudalis is absent as in  
382 *Meleagris*, whereas a very large fenestra mandibularis caudalis is present in Tetraoninae.  
383 As in most other Galloanserae, the processus retroarticularis is elongate and blade-like  
384 (mediolaterally compressed).

385 Fifteen free vertebrae are present cranial to the notarium, which agrees with the  
386 number observed in other crown Galliformes. The atlas and axis are obscured by the skull.  
387 An osseous bridge connects the processus transversus to the processus articularis caudalis  
388 in cervical vertebrae three and four. A strong midline ridge also projects from the ventral  
389 surfaces of these vertebrae. This ridge is very weak in cervical vertebra five and absent in  
390 cervical vertebrae six through nine (the ventral surfaces of more caudal vertebrae are  
391 hidden). The thoracic vertebrae are mediolaterally thin, lack pneumatic foramina, and bear  
392 cuplike cotylae for the thoracic ribs. At least the last two free thoracic vertebrae have a  
393 strongly projected processus ventralis. A notarium is present and is formed by four fused  
394 thoracic vertebrae. Each of these vertebrae bears a strongly projected ventral spine, and  
395 those of the second and third vertebrae of the notarium fuse to enclose a round fenestra.

396 Ribs from the free thoracic vertebrae bear unfused uncinate processes. The ribs of the  
397 caudalmost two vertebrae of the notarium are intact, and both lack a pneumatic opening on  
398 the cranial face between the rami. The spike-like distal end of an additional rib, probably  
399 that of the 15th presacral vertebra, is partially visible. The synsacrum is rather poorly  
400 preserved. As in other galliforms the body of the synsacrum is rounded and expanded near  
401 the midpoint. The crista spinosa synsacri is quite thin.

402 A portion of the furcula is preserved, including both omal ends but lacking the  
403 apophysis. The omal portion of the scapus claviculae is subcylindrical as in Tetraoninae,  
404 unlike the condition in *Meleagris* where it is mediolaterally flattened and further bears a  
405 pneumatized excavation on the medial face. Likewise, at least along the intact portion, the  
406 scapus maintains uniform thickness as in Tetraoninae, rather than expanding as in  
407 *Meleagris* (Fig. 3.1).

408 Both scapulae are preserved in articulation and are subequal in length to the  
409 humerus. The acromion is medially deflected, in contrast to the straight condition in  
410 *Meleagris* and Tetraoninae (Fig. 5). The facies articularis humeralis is large and  
411 subcircular. No pneumatic foramina are present on the scapula. A pneumatic opening is  
412 present between the acromion and facies articularis humeralis in Tetraoninae (Fig 5.7) and  
413 present on the dorsal surface of the facies articularis humeralis in *Meleagris* (Fig 5.12). The  
414 scapular blade is curved with a thick ventral margin and a sharp dorsal margin. A small  
415 tubercle is located on the ventral margin of the scapula, as in most crown Galliformes. This  
416 differs from the condition in some Cracidae as well as in the stem galliform *Paraortygooides*  
417 *messelensis* in which this tubercle is placed on the lateral face of the scapula (see Mayr,  
418 2000).

419                   The complete left coracoid was freed from the matrix (Fig. 3.2 + 3.3). As in other  
420                   crown Galliformes, the bone is slender, bears a flat facies articularis scapularis and lacks a  
421                   processus procoracoideus and foramen nervi supracoracoidei. The processus  
422                   acrococoracoideus is not hooked. On the dorsal surface of the coracoid, a large ovoid  
423                   pneumatic fossa opens in the area of the impressio m. sternocoracoidei as in most  
424                   phasianids (absent in quails, some partridges, and junglefowl). A pronounced lip bounds  
425                   the facies articularis sternalis distally. The angulus medialis terminates in a rounded knob,  
426                   which is present but shows substantial variation in development within extant Numididae  
427                   and Phasianidae. The processus lateralis is short and triangular, more closely resembling  
428                   the condition in *Meleagris* than the well-projected process in Tetraoninae or the rounded  
429                   process in *Pucrasia*.

430                   A well-developed fossa tricipitalis dorsalis excavates the humerus, steeply  
431                   undercutting the head (Fig. 3.5). The depth of the fossa is similar to that in *Pucrasia* and  
432                   most Tetraoninae (Fig. 5.1-5.3). *Meleagris* and some grouse taxa (*Tympanuchus* and  
433                   *Centrocercus*) show a shallower fossa (Fig. 5.4), whereas Odontophoridae and many of the  
434                   polyphyletic “partridges” (e.g., *Rollulus*, *Alectoris*, *Ammoperdix*) show a much deeper  
435                   excavation. A deep incisura capitalis partially undercuts the head of the humerus. A strong  
436                   ridge formed by the distal projection of the caput humeri separates the fossa  
437                   pneumotricipitalis dorsalis from the incisura capitidis as in other crown Galliformes. The  
438                   fossa pneumotricipitalis is large, deep and subdivided by trabeculae. The sulcus  
439                   ligamentous transversus is unusually deep and well defined. A distinct, slightly raised  
440                   supracoracoideus scar marks the caudal face of the humerus. The crista deltopectoralis is  
441                   strongly ventrally inturned and comes to a thick triangular point. The distal margin of the

442 crista deltopectoralis merges abruptly with the shaft so as to create a squared outline,  
443 contrasting with the typical condition in Phasianidae in which the crest merges more  
444 smoothly into the shaft. Along the caudal face of the shaft a thin, raised line marks the  
445 insertion of m. latissimus dorsi. As in most Phasianidae, the fossa m. brachialis is shallow.  
446 The tuberculum supracondylaris ventralis is a small, low triangular projection. The  
447 processus supracondylaris dorsalis takes the form of a low, compact process (more  
448 projected than in *Meleagris* and Tetraoninae). The epicondylaris ventralis bears a deep  
449 circular depression on its distal face. The processus flexorius is weakly projected.

450 The ulna is quite straight as preserved (Fig. 3.6+3.7), as opposed to the more bowed  
451 shape in Tetraoninae and *Pucrasia macrolopha* (*Meleagris gallopavo* shows significant  
452 variation). However, this may be at least in part an artifact of crushing. Though somewhat  
453 obscured by deformation, an ovoid impressio brachialis can be identified on the ventral face  
454 of the ulna. The impressio scapulotricipitalis is ovoid and slightly depressed. Feather  
455 papillae are weakly raised. The incisura tendinosa is essentially absent.

456 The radius is similar in general morphology to that of other Phasianidae (Fig.  
457 3.8+3.9). The tuberculum bicipitale radii is strongly developed. A foramen opens within the  
458 depressio ligamentosa on the caudal face of the radius, which may represent an apomorphy  
459 of *Centuriavis lioae* provided it does not represent individual variation. Although this  
460 foramen is absent in almost all extant phasianid specimens we examined for this study, a  
461 similar foramen was noted in a single specimen of *Meleagris gallopavo* and two much  
462 smaller foramina were observed in this region in one specimen of *Centrocercus*  
463 *urophasianus*.

464 The radiale (Fig. 3.10+3.11) is slightly proportionally shorter in the proximo-distal  
465 dimension than in turkey or grouse. As in other crown galliforms, the dorsal end of the  
466 bone is unusually wide (Mayr, 2014). Only the crus breve of the ulnare is preserved, but it  
467 is too incomplete to provide informative observations.

468 A small element preserved in isolation appears to be a sesamoid ossification (Fig.  
469 3.12). We observed a nearly identical element near the plantar surface of the  
470 tarsometatarsus, adjacent to the joint between the tibiotarsus and tarsometatarsus, in an  
471 articulated skeleton of *Lyrurus tetrix* (AMNH 12813). The distribution of this sesamoid  
472 across Phasianidae is difficult to establish as it is presumably easily lost during  
473 skeletonization of museum specimens, but we confirmed that it is present and similar in  
474 shape in disarticulated skeletons of *Meleagris gallopavo*.

475

476 *Etymology*.—In honor of Suzanne Lio, in recognition of her support for science and tireless  
477 efforts to advance the mission of the Bruce Museum.

478

479 *Remarks.*—We note that the specimen is embedded in a beige matrix. The red color was  
480 added at some stage between discovery of the fossil and the present study in an attempt to  
481 increase contrast between the bone and matrix.

482

483 cf. *Centuriavisi liogae*

484 Figure 4

485

486 *Occurrence.*—*Machaerodus* Quarry, Cherry County, Nebraska.

487

488 *Description.*—An isolated humerus (Fig. 4.1-4.2) from the *Machaerodus* quarry closely  
489 resembles that of the *Centuriavis lioae* holotype, agreeing in general proportions, the well-  
490 developed fossa tricipitalis dorsalis, the characteristic shape of the crista deltopectoralis,  
491 and the weak processus supracondylaris dorsalis. The only notable difference is the slightly  
492 greater degree of curvature of the shaft. However, there is a prominent break line just  
493 proximal to midshaft, so it is possible the shape is exaggerated by postmortem deformation.

494 An isolated tarsometatarsus (Fig. 4.3-4.7) from the *Machaerodus* quarry represents

495 another possible specimen of *Centuriavis lioae*. The bone is slender and elongated,  
496 resembling *Pucrasia* and modern turkeys in general proportions, as opposed to the stouter  
497 tarsometatarsus of grouse. It is substantially larger than that of *Rhegminornis calobates*  
498 holotype (distal width 13.5 mm versus 9.5 mm). The eminentia intercotylaris is strongly  
499 projected and the sulcus extensorius is deep and sharply bounded on its lateral and medial  
500 margins. The hypotarsus is monocanaliculate (*sensu* Mayr, 2016b) with a single canal for  
501 the tendon of *m. flexor digitorum longus*. This tendon is fully enclosed in a bony canal in  
502 almost all Phasianidae, but instead runs through a deep sulcus in a few grouse  
503 (e.g., *Tetrastes*). The crista medialis flexoris digitorum longus is the most strongly  
504 projected of the hypotarsal crests and is continuous with a sharply hooked distal projection.  
505 A low, sharp crest is present along the plantar-medial margin of the tarsometatarsus. There  
506 is no evidence of a spur, which is present in males in *Pucrasia* and Meleagridinae, but  
507 absent in both sexes in Tetraoninae.

508 In extant phasianids, an intratendinous ossification of m. gastrocnemius typically  
509 fuses to the distal margin of the crista medialis flexoris digitorum longus and the plantar  
510 face of the tarsometatarsus over the course of ontogeny (Hudson et al., 1965). We observed  
511 that in some immature birds, this ossification is completely separated from the  
512 tarsometatarsus, and in others it is fused to the crista medialis flexoris digitorum longus, but  
513 remains unfused to the plantar surface of the tarsometatarsus (Fig. 4.8). Thus we interpret  
514 the projection in the fossil as the partially ossified portion of m. gastrocnemius, and  
515 consider this indicative of immature status.

516

517 *Materials.*—AMNH FARB 8627, right humerus; AMNH FARB 8628, left tarsometatarsus.  
518 Measurements in Table 1.

519

520 *Remarks.*—These specimens were recovered in the same quarry and potentially represent  
521 additional individuals of *Centuriavis lioae*, to which we tentatively refer them. The  
522 humerus is approximately 88% the length of the holotype humerus. This difference is well  
523 within the range of sexual dimorphism observed in extant *Pucrasia*, Meleagridinae, and  
524 Tetraonidae (in which some species show almost no size dimorphism and others show  
525 substantial levels). It is plausible that the holotype individual of *Centuriavis lioae* was male  
526 and the smaller humerus belonged to a female individual. However, the possibility that  
527 AMNH FARB 8627 belongs to a second smaller phasianid species cannot be conclusively  
528 ruled out. The relative proportions of the humerus and tarsometatarsus vary dramatically in  
529 extant Phasianidae, with the tarsometatarsus being much shorter than the humerus in many  
530 extant grouse, nearly as long as the humerus in *Pucrasia*, and slightly longer than the

531 humerus in extant turkeys. We consider it more likely than not that the tarsometatarsus also  
532 belongs to *Centuriavis lioae*. However, because no major leg bones are preserved in the  
533 holotype, conclusive referral of AMNH FARB 8628 to this species or a separate taxon will  
534 have to await discovery of more complete associated specimens.  
535

536

537 **Phasianid Neuroanatomy**

538

539 Avian endocasts have been shown to be faithful proxies for the volume and surface  
540 morphology of the brain (Iwaniuk and Nelson, 2002; Watanabe et al., 2019; Early et al.,  
541 2020a). However, fossil endocasts remain relatively rare, as few avian fossils preserve the  
542 skull and in those that do, the braincase is often flattened so that no details of the endocast  
543 can be recovered. Thus, the well-preserved skull of *Centuriavis lioae* provides potentially  
544 valuable insight into galliform paleoneuroanatomy (Fig. 6).

545 Volumetric data for the *Centuriavis lioae* endocast were reported by Early et al.  
546 (2020b), who referred to the specimen as an unnamed Miocene galliform. The endocast is  
547 complete except for damage to the right optic lobe. In dorsal view, the cerebral hemispheres  
548 differ from those in all three sampled extant species in having a more circular shape, with  
549 less pronounced rostral tapering. As is typical of Galliformes (Bang and Cobb, 1968), the  
550 olfactory bulbs are small. The Wulst is strongly projected and most closely resembles that  
551 of *Meleagris*. In contrast, the Wulst is not as wide in *Bonasa* and only weakly projected in  
552 *Colinus* and in the Eocene-Oligocene phasianoid skull described by Mayr et al. (2021).  
553 Both extant phasianids and *Centuriavis* exhibit a pronounced vallecula running along the

554 lateral border of the Wulst, which furthermore shows caudal branching in *Meleagris* and  
555 *Bonasa*. In *Colinus*, the vallecula is not as well developed, which may be related at least in  
556 part to the smaller size of the endocast. The optic lobes in the *Centuriavis* endocast are  
557 well-developed and positioned almost entirely caudal to the widest point of the cerebral  
558 hemispheres. The degree of lateral projection (in ventral view) is similar to that in  
559 *Meleagris*, whereas the optic lobes project farther laterally in *Bonasa* and *Colinus*.

560 The cerebellum of *Centuriavis* is complete except for the caudal margin. The  
561 cerebellar folia are strongly defined, most similar to the condition in *Colinus*. The folia are  
562 slightly less well-defined in *Bonasa* and relatively poorly defined in *Meleagris*. A  
563 pronounced sinus occipitalis runs along the midline of the cerebellum in all four taxa  
564 sampled here, but is weaker in *Colinus* than in the phasianids. The floccular lobes are large  
565 and project from body of the cerebellum at an approximately 45-degree angle, and are  
566 intermediate in relative width to those of *Meleagris* and *Bonasa*.

567

568

## 569 **Phylogenetic Relationships**

570

571 When the morphological dataset is analyzed without the backbone constraint,  
572 Gallinuloididae, Megapodidae, Cracidae, and Numididae are recovered on successive  
573 branches within Pan-Galliformes. A monophyletic Odontophoridae is nested within a large  
574 polytomy of phasianid taxa, rendering Phasianidae polyphyletic.

575 The primary phylogenetic analysis using the molecular backbone constraint from  
576 the Hosner et al. (2017) study resulted in 3,642 most parsimonious trees (MPTs) of 478

577 steps. Throughout the strict consensus tree (Fig. 7), placement of taxa via morphological  
578 data appears to be largely consistent with molecular phylogenies of Galliformes.  
579 Specifically, all sampled but unconstrained species of Megapodidae, Cracidae, Numididae,  
580 Odontophoridae, and Phasianidae were recovered in their “correct” family (i.e. matching  
581 their placement in molecular phylogenies with larger taxonomic samples). *Gallinuloides*  
582 and *Paraortygooides* were recovered as stem landfowl and *Palaeortyx* was recovered as the  
583 sister taxon to Odontophoridae + Phasianidae. *Centuriavis* and *Panraogallus* were  
584 recovered within Phasianidae, as part of a large polytomy including turkeys, grouse,  
585 *Pucrasia*, *Perdix*, and several other phasianids. This polytomy is primarily due to the  
586 instability of *Panraogallus*, which is equally parsimonious to place as a stem turkey, a stem  
587 grouse, or elsewhere in Phasianidae (e.g. as a close relative of *Chrysolophus*).

588 Following exclusion of *Panraogallus*, the second analysis resulted in 1,816 MPTs of  
589 474 steps. In the strict consensus tree (Fig. 8), relationships are better resolved in  
590 Phasianidae. *Centuriavis* is recovered as part of a polytomy with *Pucrasia* and a clade  
591 uniting Tetraoninae + Meleagridinae. Due to incomplete preservation in *Centuriavis*,  
592 substantial differences in skeletal anatomy of grouse and turkeys, and lack of resolution of  
593 the position of *Centuriavis* relative to *Pucrasia*, only a single unambiguous character can be  
594 resolved as a synapomorphy of the clade uniting *Pucrasia*, *Centuriavis*, Meleagridinae and  
595 Tetraoninae. This character (60:1, furcula facet of coracoid with strong concavity in caudal  
596 margin) is further secondarily reversed in Tetraoninae. The most convincing character  
597 uniting turkeys and grouse to the exclusion of *Centuriavis* and *Pucrasia* is the shape of the  
598 acromion (character 55), which is strongly medially deflected in *Centuriavis* and *Pucrasia*  
599 as in most Phasianidae, but straight in grouse and turkeys (Fig. 4). Grouse and turkeys also

600 share complete fusion of the uncinate processes to the ribs (character 40: unfused in  
601 *Centuriavis* and *Pucrasia*), though this feature is also convergently present in many other  
602 phasianids. Because the femur is not preserved in *Centuriavis*, it is uncertain if limb bone  
603 proportions (91:0, humerus exceeds femur in length) represent a synapomorphy of the  
604 grouse + turkey clade or instead support a sister group relationship between *Centuriavis*  
605 and the grouse + turkey clade to the exclusion of *Pucrasia*.

606 Monophyly of crown Meleagridinae is supported by nine unambiguous  
607 synapomorphies in our results, most of which show some degree of homoplasy: (7:1)  
608 lacrimal forming sharply projecting supraorbital spine (convergently evolved in several  
609 other phasianid lineages), (43:1) scapus claviculae of furcula maintains uniform width near  
610 omal end (convergently evolved in Pavoninae), (53:1) incisurae medialis et lateralis of  
611 sternum shallow, (65:1) facies articularis sternalis of coracoid bounded by strong ridge  
612 (convergently evolved in several other phasianid lineages), (68:0) weakly developed fossa  
613 pneumotricipitalis dorsalis (convergently evolved in the grouse *Tympanuchus* and  
614 *Centrocercus*, as well as *Polyplectron*), (93:1) crista cnemialis cranialis forming strong  
615 triangular point in cranial view (convergently evolved in several other phasianid lineages),  
616 (107:1) head largely featherless (also present in *Argusianus*), (126:1) presence of frontal  
617 caruncle (snood), and (127:1) presence of a single neck wattle.

618 Monophyly of crown Tetraoninae is supported by nine unambiguous characters:  
619 (29:1) presence of fenestra mandibularis caudalis (convergently evolved in *Perdix*,  
620 *Ithaginus* and some Coturnicinae), (58:1) presence of a pneumatic foramen between the  
621 acromion and facies articularis humeralis of the scapula (convergently evolved in  
622 Pavoninae), (72:1) strong projection of the condylus ventralis of the humerus, (85:1)

623 reduction of the tuberculum preacetabulare (convergently evolved in *Arborophila*,  
624 *Polyplectron*, *Ammoperdix*), (88:0) shallow recessus caudalis fossa of pelvis (convergently  
625 evolved in *Rollulus* and some *Coturnicinae*), (89:1) wide and shallow ischium, (98:0) loss  
626 of tarsometatarsal spur (convergently lost in *Arborophilinae*, *Perdix* and some  
627 *Coturnicinae*), (120:1) feathered tarsus, and (123:1) presence of a fleshy comb above the  
628 eye.

629 We were unable to fully resolve the phylogenetic position of *Panraogallus*. This  
630 Miocene species is represented by an exceptional skeleton with intact tracheal rings  
631 indicating the trachea was longer than the bird's entire body (Li et al., 2018). Elongated  
632 trachea occur today in the extant grouse *Tetrao urogallus* and *Lagopus mutus*, many  
633 Cracidae, and the numidid *Guttera plumifera*. It is tempting to speculate that *Panraogallus*  
634 falls close to the grouse + turkey clade, as it shares an unhooked acromion with these taxa.  
635 Unfortunately, key features of the humerus and pelvis are obscured by preservation in  
636 *Panraogallus*, precluding better resolution of its phylogenetic affinities. Interestingly, the  
637 alular digit bears a distal phalanx in most Phasianidae, with development varying from a  
638 claw-like element (e.g., in Pavoninae) to a rudimentary button-like ossicle (e.g., in *Perdix*  
639 and *Pucrasia*). We found this claw to be absent in grouse and in all *Meleagris gallopavo*  
640 specimens we examined. However, we observed a rudimentary claw in some specimens of  
641 *Meleagris ocellata*. There is no distal phalanx preserved in *Panraogallus*, which would be  
642 consistent with a placement as a stem member of either the grouse or grouse + turkey  
643 lineage. However, because this small element is easily lost in macerated skeletons, the  
644 possibility it was not preserved (or even destroyed during preparation) in the fossil cannot  
645 be ignored.

646 Resolving the relationships of the small fossil galliform *Palaeortyx gallica* provides  
647 additional information on the timing of the galliform radiation. Oligocene specimens of  
648 *Palaeortyx* potentially represent the oldest record of crown Galliformes, pending better  
649 material of some poorly known taxa. Similarities in the humerus morphology of *Palaeortyx*  
650 and modern New World quail led Milne-Edwards (1867–1871) to assign the fossil taxon to  
651 Odontophoridae. As understanding of galliform phylogeny has improved, it has become  
652 clear that these similarities are likely either primitive or convergent features. Mayr et al.  
653 (2006) hypothesized that *Palaeortyx* instead represents the sister taxon to Odontophoridae  
654 and Phasianidae. Zelenkov (2019) argued for a more nested position, depicting *Palaeortyx*  
655 as the sister taxon to crown Phasianidae. Our results support the more stemward placement,  
656 resolving *Palaeortyx* as sister taxon to Odontophoridae + Phasianidae. Characters  
657 supporting the sister group relationship between *Palaeortyx* and Odontophoridae +  
658 Phasianidae include (53:1) deep incisurae in caudal margin of sternum and (76:1) presence  
659 of a large processus intermetacarpalis. However, *Palaeortyx* retains primitive limb bone  
660 proportions that support its exclusion from total-group Phasianidae. As in Anseriformes,  
661 stem Galliformes, most Megapodidae, Cracidae, and most Numididae, the humerus of  
662 *Palaeortyx* is longer than the femur (90:0), albeit only slightly so. In contrast, the femur is  
663 longer than the humerus in Odontophoridae and almost all Phasianidae, the exceptions  
664 being very large species such as turkeys, grouse, and some peafowl. In addition, the sulcus  
665 for the tendon of m. flexor hallucis longus faces plantarly in *Palaeortyx*, as in  
666 Megapodidae, Cracidae, and Numididae (character state 95:0), whereas this sulcus is  
667 oriented laterally and bounded by a well-developed crest in Odontophoridae and most  
668 Phasianidae (Mayr, 2015). In favor of the more nested placement, Zelenkov (2019) noted

669 that the proximal margin of the rim of the trochlea carpalis is only weakly notched in  
670 Odontophoridae, whereas it is more strongly notched in *Palaeortyx* and Phasianidae. In our  
671 matrix, character 74 only considers the presence or absence of this notch, which we scored  
672 as “present” in Odontophoridae, *Palaeortyx*, and Phasianidae. However, we note that  
673 editing our scoring for Odontophoridae to “absent” to reflect this alternate interpretation  
674 does not alter the result of the phylogenetic analysis.

675

## 676 **Discussion**

677

678 Through a combination of territoriality and inattention to basic taxonomic research,  
679 a large number of important avian fossils linger unstudied in museum collections. Despite  
680 its exquisite preservation, the holotype of *Centuriavis lioae* remained undescribed for  
681 nearly a century. Formal description of the species opens a window into the assembly of the  
682 modern North American landfowl fauna. As with many avian clades, there is growing  
683 evidence for the replacement of stem taxa by crown taxa close to the Paleogene-Neogene  
684 boundary. The Paleogene stem fauna included large gallinuloidids and smaller, enigmatic  
685 taxa. It is tempting to equate these groups to the large grouse and turkeys and to the small  
686 New World Quail, respectively, of the modern North American avifauna. However, this  
687 would be premature since gallinuloidids likely had different dietary preferences than  
688 modern landfowl (Mayr and Weidig, 2004) and the smaller taxa are known only from  
689 fragmentary remains that obscure their paleoecology. Whatever their ecological roles, these  
690 stem taxa were replaced by a modern fauna composed of Cracidae, Odontophoridae,  
691 Meleagridinae, and Tetraoninae. A more complete understanding of the evolution of the

692 North American galliform fauna will require a combination of new collecting efforts to fill  
693 in the substantial gaps in the stratigraphic record and resolve the affinities of poorly known  
694 taxa like *Nanortyx* and *Rhegminornis*, and re-examination of material already in collections  
695 such as *Procrax*.

696 Although the precise position of *Centuriavis* relative to *Pucrasia* remains uncertain,  
697 the occurrence of *Centuriavis* in North America leads us to prefer a placement as sister  
698 taxon to Tetraoninae + Meleagridinae. This hypothesis is consistent with a dispersal event  
699 from Asia into North America prior to the divergence between grouse and turkeys. Previous  
700 results have suggested such a dispersal event may have occurred in the Early Miocene  
701 based on molecular divergence dates, with some grouse lineages later dispersing back and  
702 forth between North America and Europe (Persons et al., 2016; Wang et al., 2017). These  
703 analyses, however, included only extant taxa. Pliocene-Pleistocene fossils, albeit often  
704 highly incomplete, have been assigned to *Tetrao*, *Lagopus*, and *Bonasa* (e.g. Jánossy, 1974;  
705 Tyrberg, 1998; Boev, 2002; Marco, 2009). In particular, if putative European fossil records  
706 of the basally diverging *Bonasa* are correctly identified to that genus (rather than perhaps  
707 representing the similar *Tetrastes*), the possibility of a Eurasian origin of both Tetraoninae  
708 and the Tetraoninae + Meleagridinae clade would bear consideration. Under either  
709 biogeographic scenario, *Centuriavis lioae* would be too young to be a plausible ancestor of  
710 turkey and grouse, suggesting it may represent a more basally diverging taxon that  
711 coexisted with early grouse and turkeys.

712 Turkeys and large grouse such as capercaillies and Black Grouse (*Tetrao*) are among  
713 the heaviest of all volant birds. The estimated body mass of *Centuriavis lioae* is ~1.7kg,  
714 which falls close to the average size for females of the Greater Sage-Grouse based on

715 values reported by Dunning et al. (2008). It thus exceeds most extant grouse but falls short  
716 of the sizes observed in the largest grouse species and extant turkeys. Turkeys and most  
717 grouse exhibit polygynous breeding, whereas the small *Tetrastes* (hazel grouse) and  
718 *Lagopus* (ptarmigans), as well as *Pucrasia*, are monogamous breeders (De Juana, 1994;  
719 Porter, 1994). Any reconstruction of the breeding system of *Centuriavis lioae* would be  
720 speculative at this stage, though if the additional specimens confirm that the smaller  
721 referred humerus belongs to the species, it would be consistent with significant sexual  
722 dimorphism.

723

## 724 **Acknowledgements**

725 We thank Mark Norell for permitting access and permission to scan the specimen, Carl  
726 Mehling and Ruth O’Leary for facilitating loan of the holotype, and Mick Ellison for  
727 photography at the AMNH. We also thank Dan Brinkman, Rick Prum, Vanessa Rhue, and  
728 Kristof Zyskowski (YPM), Helen James and Chris Milensky (USNM), Zhiheng Li (IVPP)  
729 for providing images of *Panraogallus*, and David Steadman (FLMNH) for access to  
730 comparative material, and Ruger Porter and Larry Witmer (OU) for access to *Meleagris*  
731 scans. We thank the AMNH Microscopic and Imaging Facility for providing support for  
732 microCT scanning. This work was funded in part by NSF award DEB 1655736 (to D.T.K.),  
733 NSF GRFP DGE1060934 and DGE 1645419 (to C.M.E.), and NSF DEB 1801224 (to  
734 A.M.B.).

735

## 736 **Accessibility of supplemental data**

737 The morphological matrix utilized in this study is available as a supplemental data file.

738

739

740 **References**

741 Balanoff, A.M., Bever, G.S., Colbert, M.W., Clarke, J.A., Field, D.J., Gignac, P.M., Ksepka, D.T.,  
742 Ridgely, R.C., Smith, N.A., Torres, C.R., Walsh, S., and Witmer, L.M., 2016, Best  
743 practices for digitally constructing endocranial casts: examples from birds and their  
744 dinosaurian relatives: *J Anat*, v. 229, p. 173-190.

745 Bang, B., and Cobb, S., 1968, The size of the olfactory bulb in 108 species of birds: *Auk*, v. 85, p.  
746 55-61.

747 Boev, Z. N., 2002, Tetraonidae Vigors, 1825 (Galliformes - Aves) in the Neogene-Quaternary  
748 record of Bulgaria and the origin and evolution of the family: *Acta Zoologica Cracoviensia*,  
749 v. 45, p. 263-282.

750 Boon, W.-M., Robinet, O., Rawlence, N., Bretagnolle, V., Norman, J. A., Christidis, L., and  
751 Chambers, G. K., 2008, Morphological, behavioural and genetic differentiation within the  
752 Horned Parakeet (*Eunymphicus cornutus*) and its affinities to *Cyanoramphus* and  
753 *Prosopeia*: *Emu*, v. 108, p. 251-260.

754 Bocheński, Z. M., and Campbell, K. E., 2006, The extinct California turkey, *Meleagris californica*,  
755 from Rancho La Brea: comparative osteology and systematics: Contributions in Science of  
756 the Natural History Museum of Los Angeles County v. 509, p 1-92.

757 Brodkorb, P., 1964, Catalog of Fossil Birds. Part 2 (Anseriformes through Galliformes): Bulletin of  
758 the Florida State Museum Biological Sciences, v. 8, p. 195-335.

759 Clarke, J. A., 2004, Morphology, phylogenetic taxonomy, and systematics of *Ichthyornis* and  
760 *Apatornis* (Avialae: Ornithurae): Bulletin of the American Museum of Natural History, v.  
761 2004, p. 1-179.

762 Crowe, T. M., Bowie, R. C. K., Bloomer, P., Mandiwana, T. G., Hedderson, T. A. J., Randi, E.,  
763 Pereira, S. L., and Wakeling, J., 2006, Phylogenetics, biogeography and classification of,  
764 and character evolution in, gamebirds (Aves: Galliformes): effects of character exclusion,  
765 data partitioning and missing data: Cladistics, v. 22, p. 495-532.

766 Crowe, T. M., and Short, L. L., 1992, A new gallinaceous bird from the Oligocene of Nebraska,  
767 with comments on the phylogenetic position of Gallinuloididae: Natural History Museum  
768 of Los Angeles County, Science Series v. 36, p. 179-185.

769 De Juana, E., 1994, Family Tetraonidae (grouse), pp In: , *in* del Hoyo, J., Elliot, A., and Sargatal,  
770 J., eds., Handbook of the Birds of the World Volume 2: New World Vultures to  
771 Guineafowl : Barcelona, Lynx Edicions, p. 376-411.

772 Del Hoyo, J., Elliot, A., and Sargatal, J., 1994, Handbook of the Birds of the World Volume 2:  
773 New World Vultures to Guineafowl, Barcelona, Lynx Edicions, 638p.

774 Dimcheff, D. E., Drovetski, S. V., and Mindell, D. P., 2002, Phylogeny of Tetraoninae and other  
775 galliform birds using mitochondrial 12S and ND2 genes: Molecular phylogenetics and  
776 evolution, v. 24, p. 203-215.

777 Drovetski, S. V., 2003, Plio-Pleistocene climatic oscillations, Holarctic biogeography and  
778 speciation in an avian subfamily: Journal of Biogeography, v. 30, p. 1173-1181.

779 Dunning Jr., J. B., 2008, CRC Handbook of Avian Body Masses, 2nd Edition, Boca Raton, CRC  
780 Press, 666p.

781 Dyke, G. J., Gulas, B. E., and Crowe, T. M., 2003, Suprageneric relationships of galliform birds  
782 (Aves, Galliformes): a cladistic analysis of morphological characters: *Zoological Journal of*  
783 *the Linnean Society*, v. 137, p. 227-244.

784 Early, C. M., Iwaniuk, A. N., Ridgely, R. C., and Witmer, L. M., 2020a, Endocast structures are  
785 reliable proxies for the sizes of corresponding regions of the brain in extant birds: *Journal*  
786 *of Anatomy*, v. 237, p. 1162-1176.

787 Early, C. M., Ridgely, R. C., and Witmer, L. M., 2020b, Beyond endocasts: using predicted brain-  
788 structure volumes of extinct birds to assess neuroanatomical and behavioral inferences:  
789 *Diversity*, v. 12, p. 34.

790 Emslie, S. D., 1998, Avian community, climate, and sea-level changes in the Plio-Pleistocene of  
791 the Florida peninsula: *Ornithological Monographs*, v. 50, p. 1-113.

792 Elzanowski, A., Paul, G. S., and Stidham, T. A., 2001, An avian quadrate from the Late Cretaceous  
793 Lance formation of Wyoming: *Journal of Vertebrate Paleontology*, v. 20, p. 712-719.

794 Fremd, T. J., 2010, Guidebook: SVP Field Symposium 2010 John Day Basin Field Conference.

795 Gill, F., Donsker, D., Rasmussen, P., and . 2021, IOC World Bird List. 202:  
796 <https://www.worldbirdnames.org/new/>.

797 Horsfield, T., 1821, XIV. Systematic arrangement and description of birds from the island of Java:  
798 *Transactions of the Linnean Society of London*, v. 1, p. 133-200.

799 Hosner, P. A., Tobias, J. A., Braun, E. L., and Kimball, R. T., 2017, How do seemingly non-vagile  
800 clades accomplish trans-marine dispersal? Trait and dispersal evolution in the landfowl  
801 (Aves: Galliformes): *Proceedings of the Royal Society B: Biological Sciences*, v. 284, p.  
802 20170210.

803 Hudson, G. E., Wang, S. Y. C., and Provost, E. E., 1965, Ontogeny of the supernumerary  
804       sesamoids in the leg muscles of the ring-necked pheasant: *The Auk*, v. 82, p. 427-437.

805 Iwaniuk, A., and Nelson, J., 2002, Can Endocranial volume be used as an estimate of brain size in  
806       birds?: *Canadian Journal of Zoology*, v. 80, p. 16-23.

807 Iwaniuk, A. N., and Wylie, D. R. W., 2006, The evolution of steropsis and the Wulst in  
808       caprimulgiform birds: a comparative analysis: *Journal of Comparative Physiology A*, v.  
809       192, p. 1313-1326.

810 Jánossy, D., 1974, Die mittelpaleozäne Vogelfauna von Hundsheim (Niederösterreich):  
811       Sitzungsberichte der Österreichischen Akademie der Wissenschaften, Mathematisch-  
812       Naturwissenschaftliche Klasse, Abteilung I, v. 182, p. 211-257.

813 Johnsgard, P. A., 1986, *The Pheasants of the World*, Oxford, Oxford University Press.

814 Kaiser, V. B., van Tuinen, M., and Ellegren, H., 2007, Insertion events of CR1 retrotransposable  
815       elements elucidate the phylogenetic branching order in galliform birds: *Molecular biology*  
816       and evolution, v. 24, p. 338-347.

817 Kan, X., Yang, J., Li, X., Chen, L., Lei, Z., Wang, M., Qian, C., Gao, H., and Yang, Z., 2010,  
818       Phylogeny of major lineages of galliform birds (Aves: Galliformes) based on complete  
819       mitochondrial genomes.

820 Kimball, R. T., and Braun, E. L., 2008, A multigene phylogeny of Galliformes supports a single  
821       origin of erectile ability in non-feathered facial traits: *Journal of Avian Biology*, v. 39, p.  
822       438-445.

823 Kimball, R., Braun, E., Zwartjes, P., Crowe, T., and Ligon, J., 1999, A molecular phylogeny of the  
824       pheasants and partridges suggests that these lineages are not monophyletic: *Molecular*  
825       phylogenetics and evolution, v. 11, p. 38-54.

826 Kimball, R. T., Mary, C. M. S., and Braun, E. L., 2011, A macroevolutionary perspective on  
827 multiple sexual traits in the Phasianidae (Galliformes): International Journal of  
828 Evolutionary Biology, v. 2011.

829 Kriegs, J. O., Matzke, A., Churakov, G., Kuritzin, A., Mayr, G., Brosius, J., and Schmitz, J., 2007,  
830 Waves of genomic hitchhikers shed light on the evolution of gamebirds (Aves:  
831 Galliformes): BMC Evolutionary Biology, v. 7, p. 1-11.

832 Ksepka, D. T., 2009, Broken gears in the avian molecular clock: new phylogenetic analyses  
833 support stem galliform status for *Gallinuloides wyomingensis* and rallid affinities for  
834 *Amitabha urbsinterdictensis*: Cladistics, v. 25, p. 173-197.

835 Lander, E. B., 2008, Early Clarendonian (late middle Miocene) fossil land mammal assemblages  
836 from the Lake Mathews Formation, Riverside County, southern California, and a  
837 preliminary review of *Merychyus* (Mammalia, Artiodactyla, Oreodontidae): Geology and  
838 Vertebrate Paleontology of Western and Southern North America: Contributions in Honor  
839 of David P. Whistler. Natural History Museum of Los Angeles County Science Series, v.  
840 41, p. 181-212.

841 Li, Z., Clarke, J. A., Eliason, C. M., Stidham, T. A., Deng, T., and Zhou, Z., 2018, Vocal  
842 specialization through tracheal elongation in an extinct Miocene pheasant from China:  
843 Scientific Reports, v. 8, p. 8099.

844 Linnaeus, C., 1758, *Systema naturæ per regna tria naturæ, secundum classes, ordines, genera,*  
845 *species, cum characteribus, differentiis, synonymis, locis.* Tomus I. Editio decima,  
846 *reformata, Holmiæ, Salvius*, 824 p.

847 Marco, A. S., 2009, New Iberian galliforms and reappraisal of some Pliocene and Pleistocene  
848 Eurasian taxa: Journal of Vertebrate Paleontology, v. 29, p. 1148-1161.

849 Marsh, O. C., 1877, New fossil vertebrates.: American Journal of Science, v. 14, p. 249-256.

850 Martin, L. D., and Tate, J., 1970, A new turkey from the Pliocene of Nebraska: The Wilson  
851 Bulletin, v. 82, p. 214-218.

852 Mayr, G., 2000, A new basal galliform bird from the Middle Eocene of Messel (Hessen,  
853 Germany): Senckenbergiana Lethaea, v. 80, p. 45-57.

854 Mayr, G., 2009, Paleogene Fossil Birds, Heidelberg, Springer, 262 p.

855 Mayr, G., 2014, Comparative morphology of the radial carpal bone of neornithine birds and the  
856 phylogenetic significance of character variation: *Zoomorphology*, v. 133, p. 425-434.

857 Mayr, G., 2016q, Avian evolution: the fossil record of birds and its paleobiological significance,  
858 John Wiley & Sons.

859 Mayr, G., 2016b, Variations in the hypotarsus morphology of birds and their evolutionary  
860 significance: *Acta Zoologica*, v. 97, p. 196-210.

861 Mayr, G., Goedert, J. L., and Rabenstein, R., 2022, Cranium of an Eocene/Oligocene  
862 pheasant-sized galliform bird from western North America, with the description of a  
863 vascular autapomorphy of the Galliformes: *Journal of Ornithology*, v. 163, p 315-326.

864 Mayr, G., Poschmann, M., and Wuttke, M., 2006, A nearly complete skeleton of the fossil  
865 galliform bird *Palaeortyx* from the late Oligocene of Germany: *Acta Ornithologica*, v. 41,  
866 p. 129-135.

867 Mayr, G., and Weidig, I., 2004, The Early Eocene bird *Gallinuloides wyomingensis*—a stem group  
868 representative of Galliformes: *Acta Palaeontologica Polonica*, v. 49, p. 211-217.

869 Milne-Edwards, A., 1867-1871, Recherches anatomiques et paléontologiques pour servir à  
870 l'histoire des oiseaux fossiles de la France, Paris, Masson, 627 p.



894 Stidham, T. A., Townsend, K., and Holroyd, P. A., 2020, Evidence for wide dispersal in a stem  
895 galliform clade from a new small-sized Middle Eocene Pangalliform (Aves: Paraortygidae)  
896 from the Uinta Basin of Utah (USA): *Diversity*, v. 12, no. 3, p. 90.

897 Swofford, D. L., 2003, PAUP\*. Phylogenetic Analysis Using Parsimony (\* and Other Methods):  
898 Sunderland, Sinauer Associates.

899 Tedford, R. H., Albright III, L. B., Barnosky, A. D., Ferrusquia-Villafranca, I., Hunt Jr, R. M.,  
900 Storer, J. E., Swisher III, C. C., Voorhies, M. R., Webb, S. D., and Whistler, D. P., 2004,  
901 Mammalian biochronology of the Arikareean through Hemphillian interval (late Oligocene  
902 through early Pliocene epochs): *Late Cretaceous and Cenozoic Mammals of North*  
903 *America: Biostratigraphy and Geochronology*. Columbia University Press, New York, p.  
904 169-231.

905 Temminck, C. J., . M, 1820, *anuel d'ornithologie, ou tableau systématique des oiseaux qui se*  
906 *trouvent en Europe: précédé d'une analyse du système général d'ornithologie, et suivi d'une*  
907 *table alphabétique des espèces*, Dufour.

908 Tordoff, H. B., 1951, A quail from the Oligocene of Colorado: *The Condor*, v. 53, p. 203-204.

909 Tordoff, H. B., and MacDonald, J., 1957, A new bird (family Cracidae) from the early Oligocene  
910 of South Dakota: *The Auk*, v. 74, p. 174-184.

911 Tyrberg, T., 1998, *Pleistocene birds of the palearctic: a catalogue*, Cambridge, Publications of the  
912 Nuttall Ornithological Club.

913 Wang, N., Kimball, R. T., Braun, E. L., Liang, B., and Zhang, Z., 2013, Assessing phylogenetic  
914 relationships among Galliformes: a multigene phylogeny with expanded taxon sampling in  
915 Phasianidae: *PloS one*, v. 8, p. e64312.

916 Watanabe, A., Gignac, P. M., Balanoff, A. M., Green, T. L., Kley, N. J., and Norell, M. A., 2019,  
917       Are endocasts good proxies for brain size and shape in archosaurs throughout ontogeny?:  
918       Journal of anatomy, v. 234, p. 291-305.

919 Weigel, R. D., 1963, Oligocene birds from Saskatchewan: Quarterly Journal of the Florida  
920       Academy of Sciences, v. 26, p. 257-262.

921 Wetmore, A., 1943, Fossil birds from the Tertiary deposits of Florida: Proceedings of the New  
922       England Zoological Club, v. 22, p. 59-68.

923 Wetmore, A., 1956, A fossil guan from the Oligocene of South Dakota: Condor, v. 58, p. 234-235.

924 Zelenkov, N. V., and Panteleyev, A. V., 2019, A small stem-galliform bird (Aves: Paraortygidae)  
925       from the Eocene of Uzbekistan: Comptes Rendus Palevol, v. 18, p. 517-523.

926 Zusi, R. L., and Livezey, B. C., 2000, Homology and phylogenetic implications of some enigmatic  
927       cranial features in galliform and anseriform birds: Annals of Carnegie Museum, v. 69, p.  
928       157-193.

929 **Appendix: Phylogenetic character list (newly added characters marked**  
930 **with asterisk)**

931

932 *Osteology*

- 933 1. Rostrum: (0) dorsoventrally shallow; (1) dorsoventrally deep.
- 934 2. Beak, spatulate shape in dorsal view: (0) absent; (1) present.
- 935 3. Width of pila supranasalis between external nares: (0) wide; (1) narrow.
- 936 4\*. Premaxilla, processus nasalis: (0) divides rostral portion of frontal; (1) does not divide  
937 rostral portion of frontal.
- 938 5\*. Premaxilla, processus nasalis: (0) left and right premaxilla remain separate along  
939 midline of internarial bar; (1) left and right premaxilla fused along internarial bar.
- 940 6. Nasal septum: (0) absent; (1) present.
- 941 7. Lacrimal, processus supraorbitalis: (0) no caudal projection into orbit, or weak and blunt  
942 projection; (1) forms a sharp spine projecting into orbit.
- 943 8. Lacrimal, facies articularis frontonasalis in dorsal view: (0) contact with frontal forms a  
944 straight suture; (1) lacrimal occupies a notch in lateral margin of frontal.
- 945 9. Ectethmoid: (0) present; (1) highly reduced or lost.
- 946 10. Maxillopalatine shelf: (0) absent; (1) present.
- 947 11. Palatine and pterygoid: (0) fused; (1) separate.
- 948 12. Processus postorbitalis: (0) short; (1) greatly elongated.
- 949 13. Processus zygomaticus: (0) well-developed; (1) absent or poorly-developed; (2)  
950 processus zygomaticus short, but continuous with well-ossified aponeurosis zygomatica  
951 which extends rostral to near or beyond the level of the postorbital process.

952 14. Processus postorbitalis and processus zygomaticus (including aponeuroses if present):  
953 (0) unfused; (1) fused distally.

954 15. Rounded flange projecting ventrally from dorsal margin of tympanic region: (0) absent  
955 or weak; (1) strongly developed. See Figure 7 of Ksepka (2009).

956 16. Processus basipterygoideus: (0) long and arising caudally; (1) short and arising rostrally  
957 on parasphenoid rostrum.

958 17. Quadratojugal-quadratae articulation: (0) quadratojugal articulates at the level of the  
959 ventral extent of the condylus caudalis; (1) quadratojugal articulates well dorsal to the level  
960 of the condylus caudalis.

961 18\*. Quadratae, cotylaris quadratojugalis: (0) complete; (1) with notch in caudal rim.

962 19\*. Quadratae, capitulum oticum and capitulum squamosum: (0) widely separated; (1)  
963 nearly in contact, (2) merged.

964 20. Quadratae, processus orbitalis: (0) short; (1) long.

965 21\*. Quadratae, strongly projected tubercle on caudal surface of processus oticus, just dorsal  
966 of processus mandibularis: (0) absent; (1) present.

967 22\*. Quadratae, tubercle on ventral margin of processus opticus: absent (0); present (1).

968 23\*. Quadratae, foramen pneumaticum caudomediale: (0) absent; (1) present.

969 24\*. Quadratae, foramen pneumaticum rostromediale: (0) absent; (1) present.

970 25\*. Quadratae, foramen pneumaticum basiorbitale: (0) absent; (1) present.

971 26\*. Quadratae, articulation for mandible: (0) three condyles; (1) bicondylar.

972 27. Mandible, processus coronoideus: (0) absent or poorly developed; (1) strongly  
973 projected.

974 28. Mandible, deep groove on ventral surface of symphysis: (0) absent; (1) present .

975 29. Mandible, fenestra mandibularis caudalis: (0) absent; (1) present.

976 30. Mandible, two strong grooves on ventral surface of symphysis: (0) absent; (1) present.

977 31\*. Mandible, processus retroarticularis: (0) absent; (1) present.

978 32\*. Mandible, processus retroarticularis: (0) unhooked; (1) hooked.

979 33\*. Mandible, processus retroarticularis: (0) narrow; (1) blade-like (dorsoventrally tall), but  
980 short; (2) blade-like and elongated.

981 34. Axis, foramina transversaria: (0) absent; (1) present.

982 35. Cervical vertebrae 3 and 4, bony bridge from processus transversus to processus  
983 articularis caudalis: (0) absent; (1) present.

984 36. Thoracic vertebrae, lateral pneumatic fossa: (0) absent; (1) present.

985 37. Notarium, degree of fusion of thoracic vertebrae: (0) partial; (1) complete.

986 38. Notarium, number of incorporated vertebrae: (0) four or less; (1) five.

987 39. Synsacrum, processes transversus of sacral vertebrae at level of acetabulum forming  
988 dorsoventrally tall lamina that contacts the medial margin of acetabulum: (0) absent; (1)  
989 present.

990 40. Processus uncinatus: (0) fused to ribs; (1) not fused to ribs; (2) absent.

991 41. Furcula: (0) U-shaped; (1) V-shaped.

992 42. Furcula, scapus claviculae: (0) stout; (1) slender.

993 43. Furcula, scapus claviculae: (0) widening towards extremitas omalis; (1) of uniform  
994 thickness (1).

995 44. Furcula, apophysis furculae: (0) small or obsolete; (1) pronounced projection.

996 45. Sternum, spina interna: (0) absent; (1) present.

997 46. Sternum, spina externa: (0) absent; (1) present.

998 47. Sternum, processus craniolateralis: (0) perpendicular to carina; (1) oriented at angle of  
999 45 degrees with respect to carina; (2) parallel to carina. Ordered.

1000 48. Sternum, processus craniolateralis: (0) short; (1) moderate length; (2) long. Ordered.

1001 49. Sternum, processus craniolateralis: (0) wide; (1) moderate width; (2) narrow.

1002 50. Sternum, apex carinae: (0) extends far cranially; (1) shifted caudally.

1003 51. Sternum, marked sulcus along cranial face of carina: (0) absent; (1) present.

1004 52. Sternum, caudal incisurae: (0) single; (1) double.

1005 53. Sternum, incisurae medialis et lateralis: (0) shallow; (1) deep.

1006 54. Sternum, caudal margin: (0) wide; (1) tapering.

1007 55. Scapula, acromion: (0) medially deflected; (1) straight.

1008 56. Scapula, facies articularis humeralis: (0) parallel to corpus scapulae; (1) acute with  
1009 respect to corpus.

1010 57. Scapula, pneumatic foramen piercing dorsal surface of facies articularis humeralis: (0)  
1011 absent; (1) present.

1012 58. Scapula, pneumatic foramen between acromion and facies articularis humeralis: (0)  
1013 absent; (1) present.

1014 59. Coracoid, cotyla scapularis: (0) cup-like, deeply excavated; (1) shallow.

1015 60\*. Coracoid, facies articularis furcularis: (0) round; (1) notched, with concavity in caudal  
1016 margin.

1017 61. Coracoid, distinctly projected processus procoracoideus: (0) absent; (1) present.

1018 62. Coracoid, foramen nervi supraceracoidei: (0) present; (1) absent.

1019 63. Coracoid, blunt ventral projection at omal end, adjacent to facies articularis clavicularis:

1020 (0) absent; (1) present.

1021 64. Coracoid, distinct fossa pneumaticum on dorsal surface: (0) absent; (1) present.

1022 65. Coracoid, facies articularis sternalis: (0) grades smoothly into dorsal surface of shaft;

1023 (1) bordered dorsally by a strong raised lip.

1024 66. Coracoid, processus lateralis: (0) rounded, with weak projection; (1) pointed, with

1025 strong projection.

1026 67. Humerus, crista bicipitalis in cranial view: (0) rounded; (1) squared.

1027 68. Humerus, fossa pneumotricipitalis dorsalis (0) rudimentary or absent; (1) moderately

1028 developed; (2) strongly developed, forming deep excavation. Ordered. *Panraogallus* was

1029 coded 0/1 as the state is uncertain due to preservation (see Li et al., 2018).

1030 69. Humerus, caudal surface, foramen pneumaticum: (0) small; (1) large; (2) absent. State

1031 (2) was added to represent the apomorphic condition in *Palaeortyx*.

1032 70. Humerus, elongate raised crest on shaft, distal to tuberculum dorsale (this crest

1033 represents an accessory insertion of the tendon of m. supracoracoideus): (0) absent; (1)

1034 present.

1035 71 Humerus, incisura capitis: (0) continuous with fossa tricipitalis dorsalis; (1) separated

1036 from fossa tricipitalis dorsalis by a ridge.

1037 72. Humerus, distal extent of condylus ventralis in cranial view: (0) not markedly extended

1038 distally; (1) markedly protrudes distally.

1039 73. Ulna: (0) shorter or equal to humerus in length; (1) longer than humerus.

1040 74. Carpometacarpus, ventral face, proximal margin of rim of trochlea carpalis: (0)

1041 smoothly rounded; (1) with small notch.

1042 75. Carpometacarpus, spatium intermetacarpale: (0) narrow; (1) wide.

1043 76. Carpometacarpus, processus intermetacarpalis: (0) absent; (1) present and overlapping  
1044 metacarpal III.

1045 77. Carpometacarpus, large bony spur projecting from cranial face of carpometacarpus: (0)  
1046 absent; (1) present.

1047 78. Carpometacarpus, cranial face: (0) flat or rounded; (1) sharp ridge present.

1048 79. Carpometacarpus, metacarpal III: (0) shaft untwisted; (1) strongly twisted.

1049 80. Alular digit, rudimentary claw: absent (0); very small and button-shaped (1); claw-like  
1050 (2). Ordered. This small claw is often lost during maceration of specimens, and so taxa that  
1051 lacked a claw were coded “?” unless true absence could be confirmed from the literature.

1052 81. Pelvis, cranial margin: (0) flared laterally; (1) not flared laterally.

1053 82. Pelvis, canalis iliosynsacralis opens caudally at two large, depressed foramina located  
1054 between the iliac crests and the crista spinosa synsacra: (0) absent; (1) present.

1055 83. Pelvis, cranially directed tab-like process placed dorsal to the antitrochanter: absent (0);  
1056 present (1).

1057 84. Pelvis, ilia and crista spinosa synsacri: (0) remain separate; (1) fused at dorsal margin.

1058 85. Pelvis, tuberculum preacetabulare (pectineal process): (0) long and projected; (1) small  
1059 point.

1060 86. Pelvis, spina dorsolateralis ilii projects as sharp mediolaterally narrow process, adjacent  
1061 to lateral margin of synsacrum and proximal caudal vertebrae: (0) absent; (1) present.

1062 87. Foramen ilioischadicum: (0) open caudally; (1) closed.

1063 88. Pelvis, recessus caudalis fossa: (0) shallow; (1) deep; (2) absent.

1064 89. Depth of ischium relative to the width of the synsacrum: (0) deep; (1) shallow and wide  
1065 (1).

1066 90. Spatium ischiopubicum: (0) dorsoventrally wide; (1) dorsoventrally narrow and slit-like  
1067 (1).

1068 91. Femur, length: (0) shorter or equal to humerus; (1) longer than humerus.

1069 92. Femur, fossa poplitea: (0) deeply recessed with pneumatic foramen/fossa; (1) not  
1070 deeply recessed, foramen variably present.

1071 93. Tibiotarsus, crista cnemialis cranialis, proximal apex: (0) flat or rounded in cranial  
1072 view; (1) pointed.

1073 94. Tarsometatarsus, passage of tendon of m. flexor digitorum longus: (0) sulcus, (1) bony  
1074 canal.

1075 \*95. Tarsometatarsus, sulcus for tendon of m. flexor hallucis longus: (0) open edge  
1076 plantarly directed, (1) open edge laterally directed. Discussed by Mayr (2016b).

1077 \*96. Tarsometatarsus, shared canal for tendons of m. flexor perforans digiti 2 and m. flexor  
1078 perforans et perforatus digiti II: absent (0); present (1). Discussed by Mayr (2016b).

1079 \*97: Tarsometatarsus, well developed crest along plantar surface (formed by fusion of  
1080 intratendinous ossification): (0) absent; (1) present.

1081 98. Tarsometatarsus, spurs in males: absent (0); present (1). This character cannot be scored  
1082 absent with certainty in fossil taxa known from small numbers of specimens, as the  
1083 possibility that males have not been sampled cannot be ruled out.

1084 99. Tarsometatarsus, foramen at distal end of shaft between trochlea metatarsi II and III: (0)  
1085 absent; (1) present.

1086 100. Tarsometatarsus, relative length of trochleae: (0) trochlea metatarsi II and IV of  
1087 similar length; (1) trochlea metatarsi II distinctly shorter than trochlea metatarsi IV.

1088 101. Tarsometatarsus, plantar side of articular surface of trochlea metatarsi III: (0)  
1089 symmetrical; (1) distinctly asymmetrical with lateral ridge protruding farther proximally  
1090 than medial ridge.

1091 102. Tarsometatarsus, trochleae: (0) splayed; (1) close together.

1092 103. Length of toes relative to tarsometatarsus: (0) short; (1) long, digit III subequal or  
1093 longer than tarsometatarsus.

1094 104. Hallux: (0) significantly shorter than remaining pedal digits; (1) greatly elongated,  
1095 approaches or exceeds other digits in length.

1096 105. Hallux: (0) incumbent (at same level as remaining pedal digits); (1) elevated, more  
1097 proximally located than remaining digits.

1098

1099 *Arthrology*

1100 106. Ligamentum postorbito-mandibulare: (0) absent; (1) present.

1101

1102 *Plumage*

1103 107. Integument of head: (0) largely feathered; (1) largely naked. *Lophura bulweri* is coded  
1104 variable, as males have a largely naked head while females have a largely feathered head.

1105 108. Single elongate ornamental plume on head: (0) absent; (1) present.

1106 109. Tuft of ornamental plumes with expanded distal ends on head: (0) absent; (1) present.

1107 110. Orbital region: (0) feathered; (1) patch of bare skin surrounds orbit.

1108 111. Body plumage black, spotted with white vermiculations: (0) absent; (1) present.

1109 112. Body plumage, black and white vertical barred plumage on flank: (0) absent; (1)  
1110 present.

1111 113. Contour feathers, downy barbules at base: (0) lack detachable nodes; (1) possess  
1112 detachable nodes.

1113 114. Wing: (0) longer than tail; (1) shorter than tail (1). *Gallus gallus* is coded 0/1 to reflect  
1114 the variation in tail length between males and females.

1115 115. Wing feathers: (0) diastataxic; (1) eutaxic (1)

1116 116. Outermost primaries: (0) unmodified; (1) tip bowed and stiffened for acoustic use (1).

1117 117. Number of tail feathers: (0) less than 16; (1) equal to or greater than 16.

1118 118. Tail shape: (0) round; (1) wedged or graduated; (2) vaulted.

1119 119. Tail feather moult: (0) irregular or bi-directional; (1) centrifugal; (2) centripetal.

1120 120. Tarsus: (0) unfeathered; (1) at least partially feathered.

1121 121. Sexual dimorphism in plumage: (0) absent; (1) slight, (2) marked.

1122 122. Integument of hatchling: (0) downy; (1) true feathers.

1123

1124 *Miscellaneous soft tissue*

1125 123. Fleshy, brightly colored comb dorsal to eye: (0) absent; (1) present.

1126 124. Lower beak, serrations on cutting edge of rhamphotheca: (0) absent; (1) present.

1127 125. Filtering lamellae: (0) absent; (1) rudimentary; (2) well-developed.

1128 126. Frontal caruncle (snood): (0) absent; (1) present.

1129 127. Single wattle formed by skin of neck: (0) absent; (1) present.

1130 128. Paired wattles formed by skin on side of face (at least in male): (0) absent; (1) present.

1131 129. Inflatable cervical air sacs: (0) absent; (1) present.

1132 130. Tracheal elongation in males: (0) absent; (1) present.

1133 131. Intromittant organ: absent (0) absent; (1) present.

1134 132. Uropygial gland: (0) naked; (1) tufted.

1135

1136 *Eggs and reproductive behavior*

1137 133. Eggshell, pinkish brown powdery covering: (0) absent; (1) present.

1138 134. Average clutch size: (0) four or more eggs; (1) two or three eggs.

1139 135. Mating system: (0) monogamous; (1) polygynous.

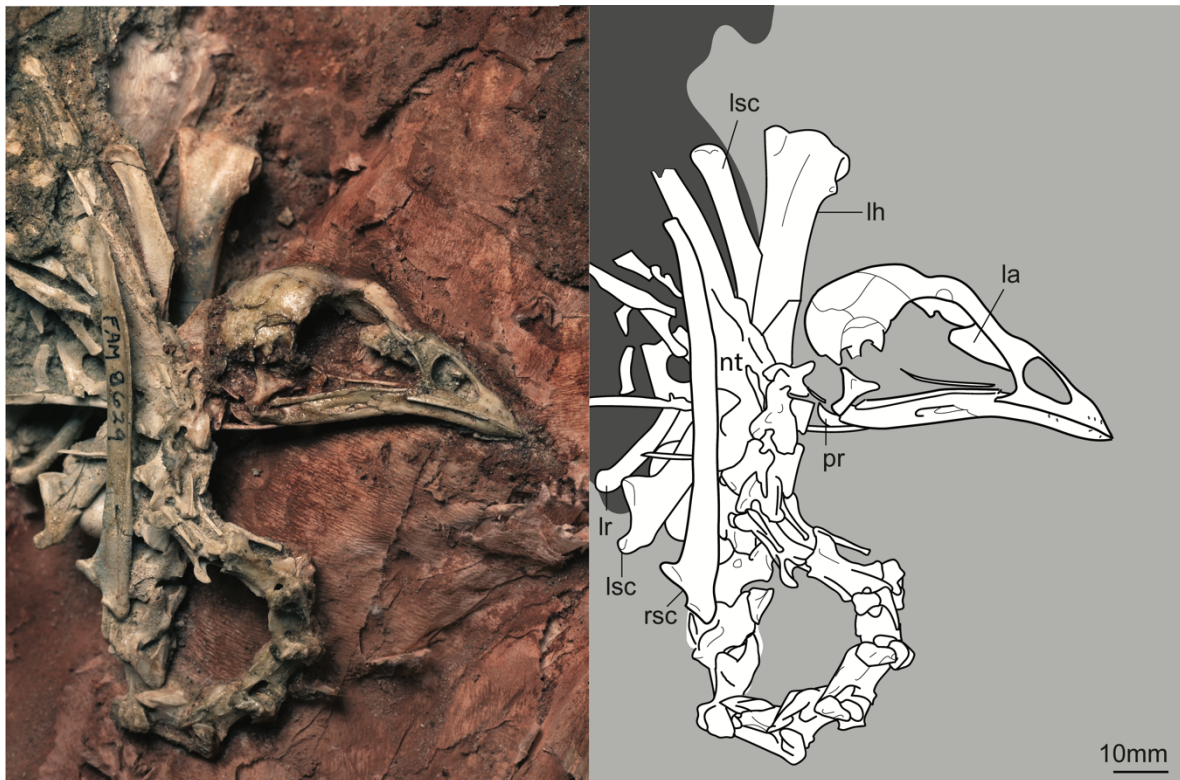
1140 136. Incubation system: (0) egg incubated by parents; (1) egg incubated by external means,

1141 e.g. geothermal heat or decaying vegetation.

1142

1143

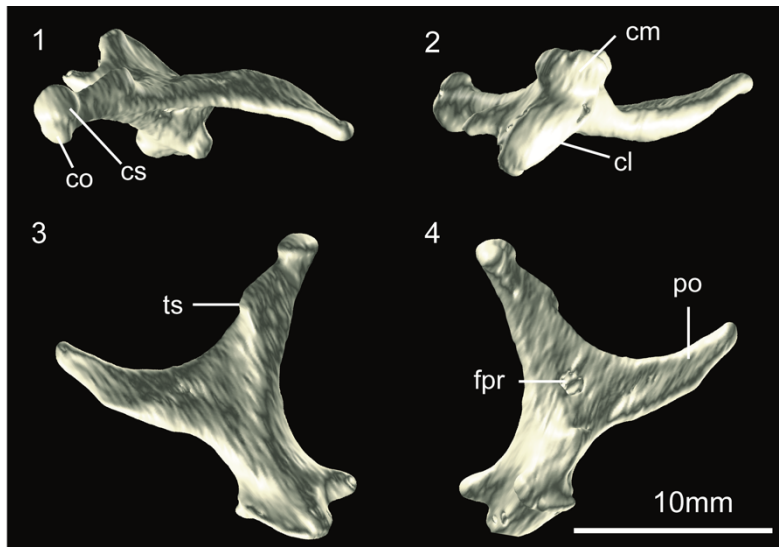
1144



1145

1146 **Figure 1.** Holotype *Centuriavis lioae* (AMNH FARB 8629). The right humerus, left  
1147 coracoid, and left radius and ulna were removed during preparation of the block.  
1148 Abbreviations: la=lacrimal, lh=left humerus, lr=left radius, lsc=left scapula, pr=processus  
1149 retroarticularis, nt=notarium, rsc=right scapula.

1150



1151

1152 **Figure 2.** CT rendering of the left quadrate of the *Centuriavis lioae* holotype (AMNH  
1153 FARB 8629) in (1) dorsal, (2) ventral, (3) lateral, (4) medial views. Abbreviations:  
1154 cl=condylus lateralis, cm=condylus medialis, co=capitulum oticum, cs=captitulum  
1155 squamosum, fpr=foramen pneumaticum rostromediale, po=processus orbitalis,  
1156 ts=tuberculum subcapitulare.



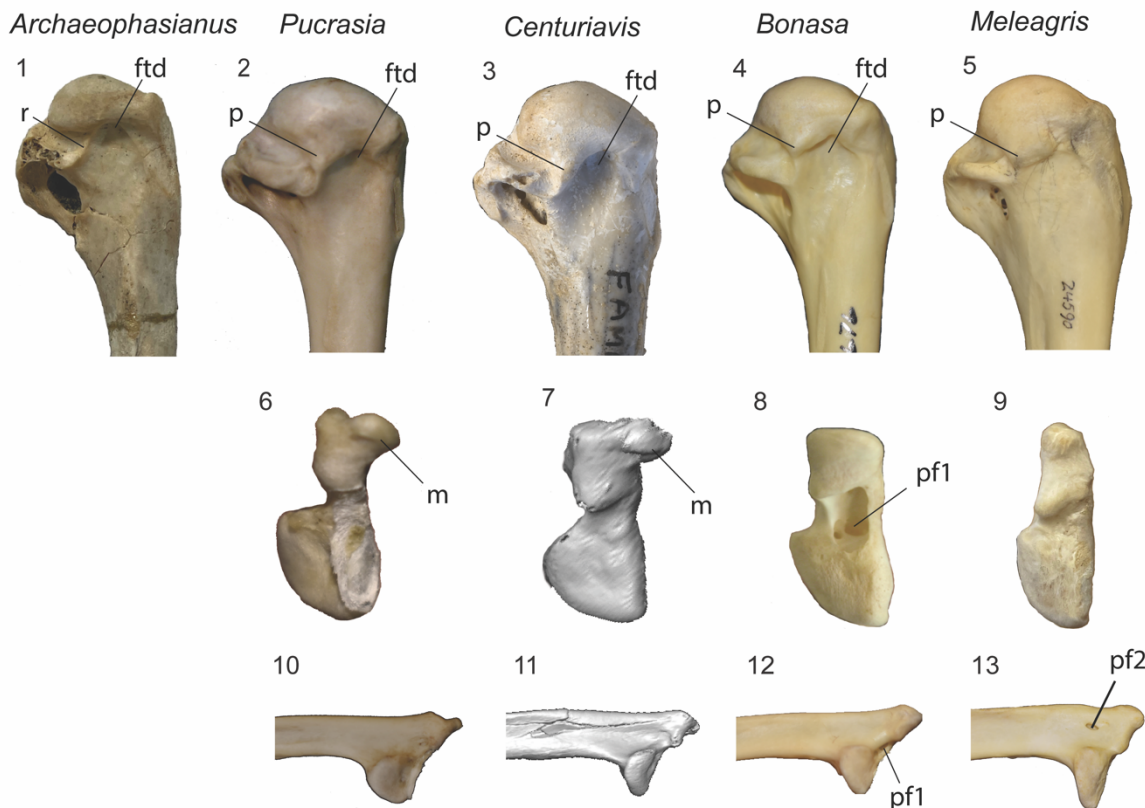
1157

1158 **Figure 3.** Postcranial elements of the *Centuriavis lioae* holotype (AMNH FARB 8629): (1) 1159 omal fragment of furcula, right coracoid in (2) ventral and (3) dorsal views, right humerus 1160 in (4) cranial and (5) caudal views, right ulna in (6) dorsal (due to crushing, the distal end is 1161 partly rotated) and (7) ventral views, right radius in (8) dorsal and (9) ventral views, right 1162 radiale in (10) cranial and (11) caudal views, and (12) sesamoid. Abbreviations: cd=crista 1163 deltopectoralis, d=damaged area, ev=epicondylaris ventralis, f=foramen, fas=faces 1164 articularis scapularis, fl=processus flexorius, fos=fossa in impressio m. sternocoracoidei,

1165 fr=facet for radius, lip=lip bounding facies articularis sternalis, ftd=fossa tricipitalis  
1166 dorsalis, kn= knob at angulis medialis; om=omal end of furcula, psd=processus  
1167 supracondylaris dorsalis, r= ridge formed by distal projection of caput humeri; sc=scar for  
1168 insertion of m. supracoracoideus, uv=notch for tendon of musculus ulnometacarpalis  
1169 ventralis.  
1170

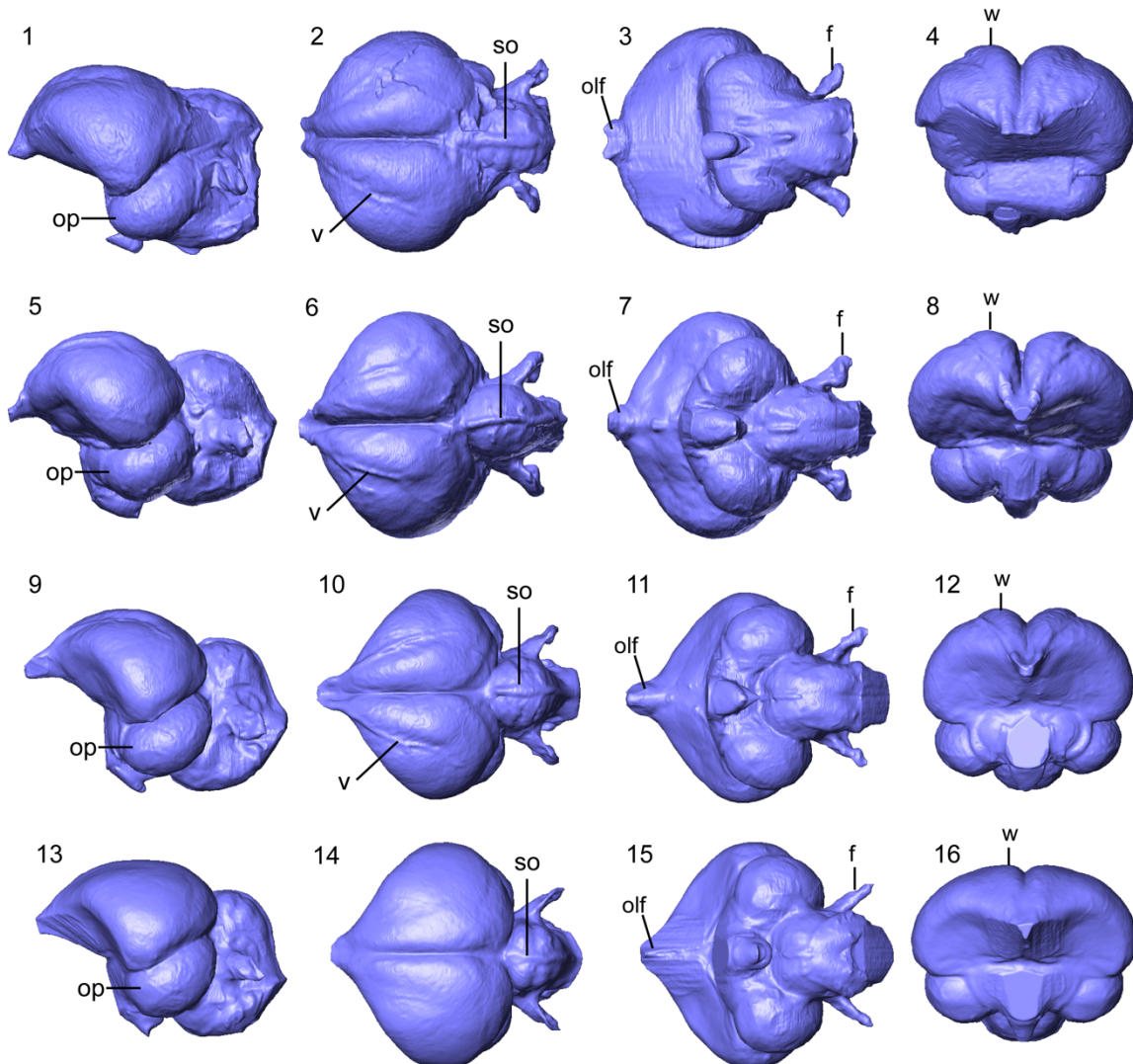


1171  
1172 **Figure 4.** Specimens of cf. *Centuriavis lioae*: (1) Cranial and (2) caudal views of small  
1173 humerus (AMNH FARB 8627). (3) Proximal, (4) distal, (5) dorsal, (6) plantar, and (7)  
1174 medial views of referred tarsometatarsus (AMNH FARB 8628) with (8) medial view of an  
1175 immature individual of the extant grouse *Bonasa umbellus* (Bruce Museum uncatalogued)  
1176 for comparison. Abbreviations: io=intratendinous ossification of m. gastrocnemius. Images  
1177 (3) and (4) are not to scale.



1178

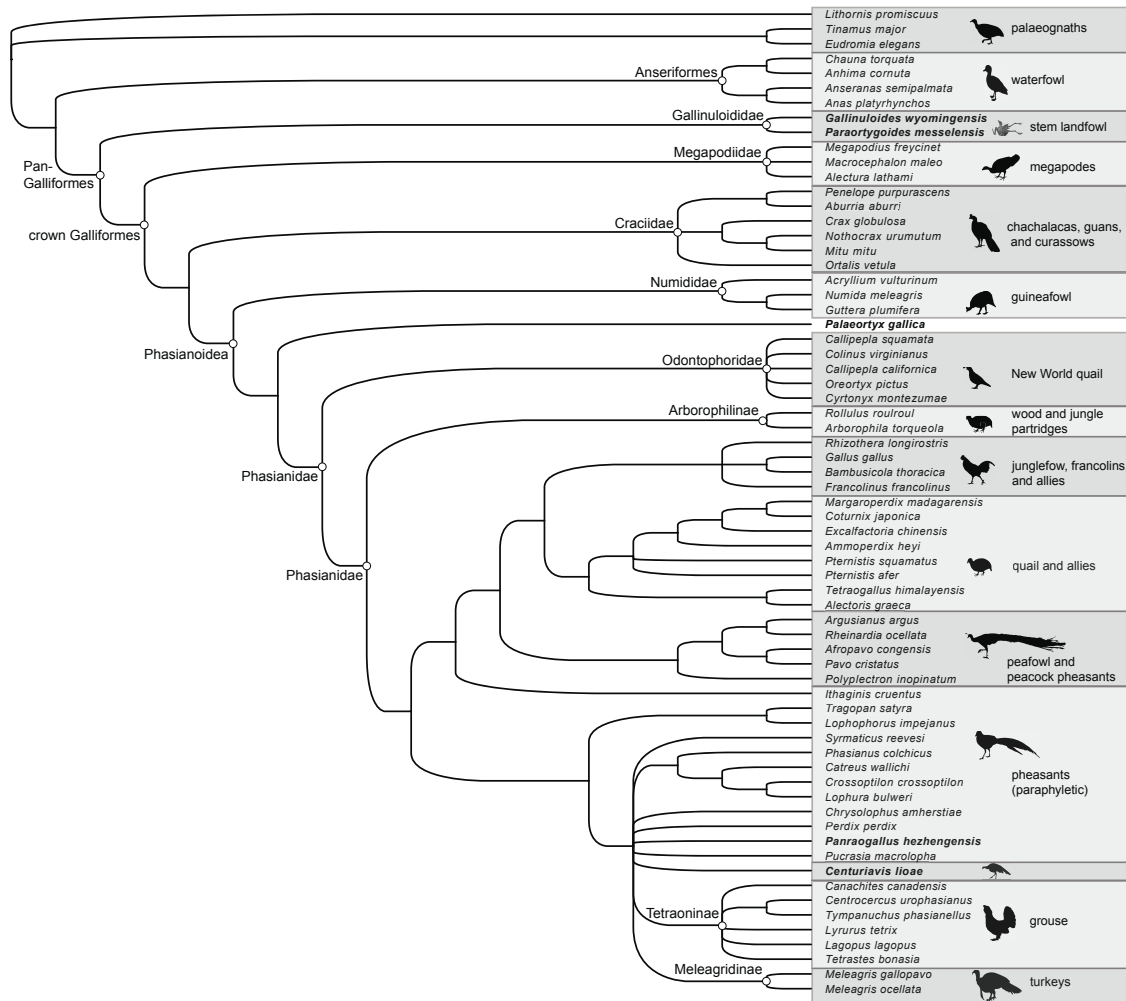
1179 **Figure 5.** Comparison of humerus and scapula of Galliformes. (1-5) Proximal end of right  
 1180 humerus is caudal view, (6-9) omal end of right scapula in lateral view, (10-13) omal end of  
 1181 right scapula is lateral view in of (1) *Archaeophasianus mioceanus* (YPM VP 909), (2,6,10)  
 1182 *Pucrasia macrolopha* (AMNH SKEL 17676), (3,7,9) *Centuriavis lioae* (AMNH FARB  
 1183 8629) (4,8,12) *Bonasa umbellus* (AMNH SKEL 21616), and (5,9,13) *Meleagris gallopavo*  
 1184 (AMNH SKEL 24590). Images (7) and (11) were taken from a CT rendering of the scapula.  
 1185 Abbreviations: ftd=fossa tricipitalis dorsalis, m=medial deflection of acromion,  
 1186 p=projection of articular surface of the caput humeri; pf1=pneumatic foramen opening  
 1187 between the acromion and facies articularis humeralis, pf2=pneumatic foramen at base of  
 1188 acromion, dorsal to facies articularis humeralis, r=weak ridge separating the fossa  
 1189 pneumotricipitalis dorsalis from the incisura capitidis. Not to scale.



1190

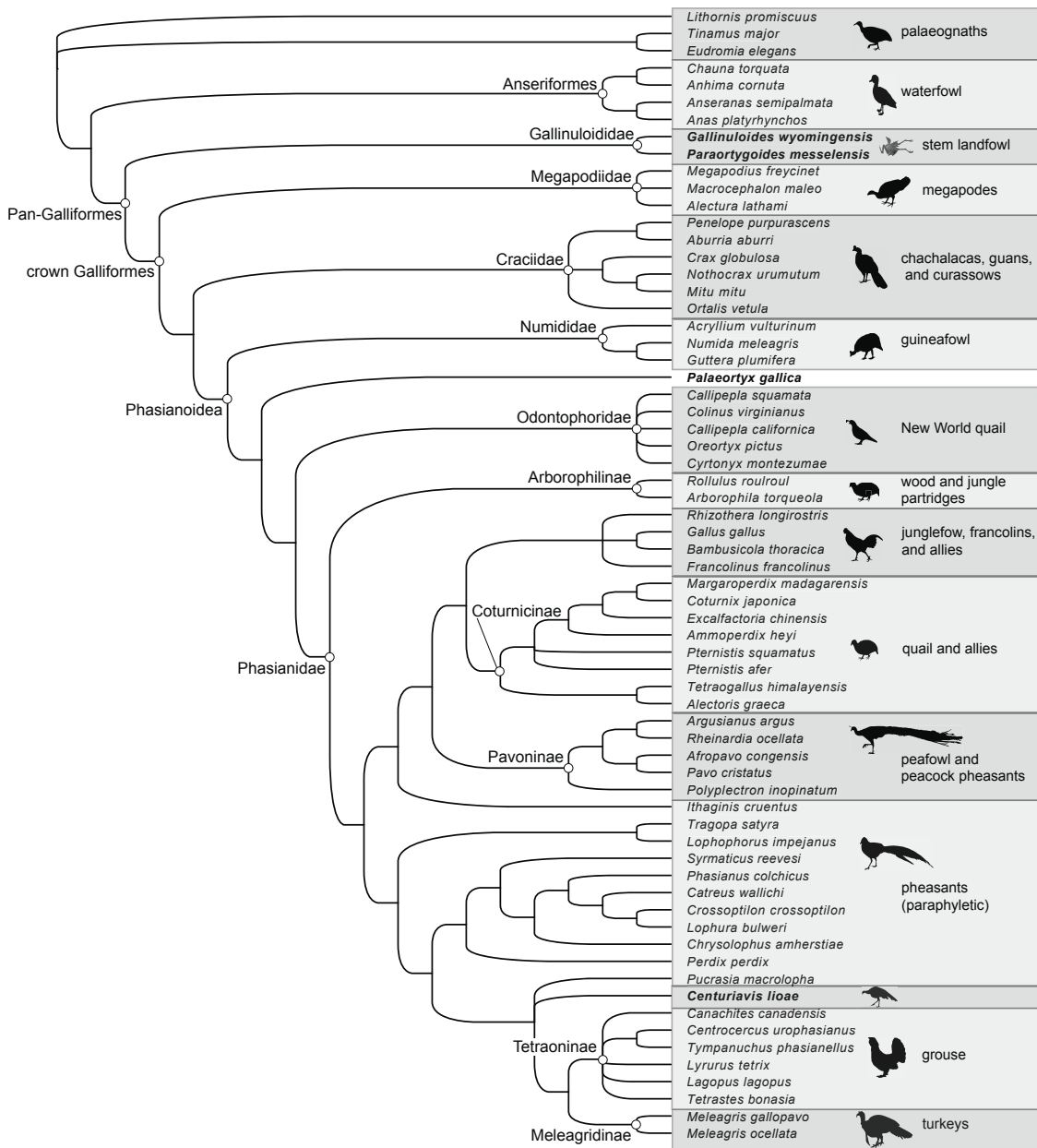
1191 **Figure 6.** Brain endocasts of North American Galliformes: *Centuriavis lioae* (AMNH  
 1192 FARB 8629) in (1) lateral, (2) dorsal, (3) ventral, and (4) rostral view. *Meleagris gallopavo*  
 1193 (OUVC 10599) in (5) lateral, (6) dorsal, (7) ventral, and (8) rostral view. *Bonasa umbellus*  
 1194 (AMNH SKEL 21616) in (9) lateral, (10) dorsal, (11) ventral, and (12) rostral view.  
 1195 *Colinus virginianus* (Odontophoridae, AMNH SKEL 2310) in (13) lateral, (14) dorsal, (15)  
 1196 ventral, and (16) rostral view. Abbreviations: f=flocular fossa, olf=olfactory bulb, op=optic  
 1197 lobe, so=sulcus olfactorius, v=vallecula, w=Wulst.

1198



1199

1200 **Figure 7.** Strict consensus of 3,642 MPTs of 478 steps from parsimony analysis of 137  
 1201 morphological characters, applying a backbone constraint based on the molecular study of  
 1202 Hosner et al. (2017). Fossil taxa are indicated in bold.



1203

1204 **Figure 8.** Strict consensus of 1,808 MPTs of 474 steps from parsimony analysis of 137  
 1205 morphological characters, excluding the fossil taxon *Panraogallus* and applying a  
 1206 backbone constraint based on the molecular study of Hosner et al. (2017). Fossil taxa are  
 1207 indicated in bold.

1208

1209 TABLE 1—Measurements (mm) from *Centuriavis lioae* holotype and referred material.

Element	Dimension	AMNH FARB 8629 (holotype)	AMNH FARB 8628	AMNH FARB 8627
Skull	length	60.0		
Scapula	length to acromion	78.9		
	length to facies articularis humeralis	69.7		
Coracoid	maximum length	60.6		
	length to midpoint of facies articularis sternalis	56.0		
Humerus	maximum length	79.8	70.5	
	proximal width	21.3	19.3	
	midshaft width	8.9	8.0	
	midshaft breadth	7.8	6.3	
	distal width	17.1	15.6	
Ulna	maximum length	81.1		
Radius	maximum length	70.3		
Tarsometatarsus	maximum length			70.2
	proximal width			13.0
	midshaft width			6.1
	midshaft breadth			12.5

1210